ENHANCEMENT OF BIOAVAILABILITY OF VITAMIN D BY NANO-SIZED DELIVERY SYSTEMS

A Thesis Submitted to
the Graduate School of Engineering and Sciences of
İzmir Institute of Technology
in Partial Fulfillment of the Requirements for the Degree of

MASTER OF SCIENCE

in Biotechnology

by
Ezgi İrem SAĞLAM

March 2023
İZMİR

ACKNOWLEDGMENTS

I would like to start by thanking my supervisor Assoc. Prof. Dr. Sevgi KILIÇ ÖZDEMİR for leading this long, educational, and challenging journey to complete my thesis. Also, I would like to thank Prof. Dr. Ekrem ÖZDEMİR for his help and opinions as another point of view. I want to thank my co-advisor Prof. Dr. Volga BULMUŞ ZAREIE and my committee members Prof. Dr. Zekiye SULTAN ALTUN, Prof. Dr. Hürriyet POLAT for their valuable comments and feedback. I also would like to thank Selen KUM ÖZŞENGEZER for conducting *in vitro* experiments. Also, I would like to thank Ayşenur Başar ÖNOL, Belgin TUNCEL and Ahmet KURUL for their kind helps and shares during experiments.

I would like to thank my lovely and caring parents Prof. Dr. Kenan SAĞLAM and Assoc. Prof. Dr. Ayşe BİRCAN for their understanding and support to get me through the challenging times with their experiences. Also, I specially thank to my little brother Jr. Dr. Hüseyin Cem SAĞLAM for always cheering me up and being there for me when I needed. Thanks for sharing my happiness with me, believing in me, and keeping me motivated through my academic journey.

I feel genuinely lucky to have a friend like İklim GÖKÇE who is miles away but right there beside me all the time. Thanks for your sisterhood, understanding and courage to new beginnings that always inspires me. I would like to thank Ataberk EGE for his love, patience, and empathy that made him think about my thesis even more than me. I am very glad that I have you in my life. Also, I would like to thank my dear friends Ezgi GÖKSOY, Özlem KARAKAYA and Pelinsu EKMEKÇİ for their endless support and love even if we are in different cities and countries.

I also thank Scientific and Technological Research Council of Turkey (TÜBİTAK) for financial support with the research grants through project number of 121M625 and 2210-C National MSc Scholarship Program in the Priority Fields in Science and Technology.

ABSTRACT

ENHANCEMENT OF BIOAVAILABILITY OF VITAMIN D BY NANO-SIZED DELIVERY SYSTEMS

Studies have indicated that Vitamin D (VitD) may decrease tumor invasiveness and propensity to metastasize. Cholecalciferol ($VitD_3$) is the passive form of $VitD_3$ and converts to active calcitriol through two-step hydroxylation reactions in the body, promoting binding to VitD-receptors (VDR). However, some breast cancer cells, especially MDA-MB-231, have very low levels of VDR. Besides, $VitD_3$ suffers from first pass-effect of the liver which causes deactivation of $VitD_3$. Therefore, new approaches are needed to increase $VitD_3$ level in the cancerous sites. In this study, $VitD_3$ was loaded into liposomes, which were subsequently coated by Fucoidan (FUC) to promote their binding to MDA-MB-231 cancer cells. Fucoidan strongly binds to P-selectins overexpressed in the breast cancer cells, blocking the cancer cells to adhere on the platelets to carry within the body, causing metastasis. Doxorubicin (DOX), being considered as the one of the most effective chemotherapeutic agents against breast cancer, was also loaded into liposomes in a similar manner. By liposomal encapsulations and fucoidan coating, it was aimed to deliver the all-cargo directly to the cancerous site and enhance the bioavailability of both agents at the target site. It was seen that liposomal $VitD_3$ was more effective than free form to inhibit cell proliferation and, therapeutic potential of DOX increased with $VitD_3$.$VitD_3$ loaded FUC coated liposomes at optimized concentrations has a comparable effect with DOX-loaded liposomes with and without FUC coating. Overall, these results suggested that $VitD_3$ and DOX loaded and FUC coated liposomes can be applied as combined therapy in cancer treatment.

ÖZET

NANO BOYUTLU TAŞIMA SİSTEMLERİ İLE D VİTAMİNİNİN BİYOYARARLANIMININ ARTTIRILMASI

Vücuda çeşitli faydaları olduğu bilinen fakat son zamanlarda KOVID-19 nedeniyle medikal çalışmalara konu olan vitamin D'nin (VitD) anti-kanser özelliği yeni bir çalışma konusudur. Birçok insanda VitD yetersizliği görülmektedir ve yapılan araştırmalara göre VitD yetersizliği çeşitli kanser tiplerinin oluşma riski ile doğru orantılıdır. MDA-MB-231 hücre hattı gibi birçok meme kanseri hücresi, VitD reseptörü (VitDR) ve VitD sentezi için gereken enzimleri barındırır.

Kolekalsiferol ($VitD_3$) VitD'nin pasif halidir ve vücutta iki aşamalı hidroksilasyon reaksiyonları yoluyla aktif kalsitriole ($VitD_2$) dönüşür. Lipozomal enkapsülasyon kullanarak $VitD_3$'ün fiziksel özellikleri geliştirilebilir ayrıca metabolik faaliyetlerden korunarak tümör hücresine daha etkili dozlarda ulaşması sağlanabilir. Doksorubisin (DOX) meme kanseri tedavilerinde kullanılan en etkili antibiyotiklerden sayılmaktadır. Fukoidan (FUC) anti-kanser etkisi olduğu bilinen sülfatlanmış bir polisakkarittir ve meme kanseri hücrelerinde bulunan P-selektinlere güçlü bir şekilde bağlanıp ve kanser hücrelerinin vücutta taşınacak trombositlere yapışmasını engeller.

Bu çalışmada $VitD_3$ ve DOX ayrı ayrı, MDA-MB-231 kanser hücrelerine bağlanmalarını desteklemek için daha sonra FUC ile kaplanan lipozomlara yüklendi. Lipozomal kapsüllemeler ve FUC kaplama ile lipozomların doğrudan kanserli bölgeye iletilmesi ve her iki ajanın da hedef bölgedeki biyoyararlanımının arttırılması amaçlanmıştır. Deneyler sonucunda, lipozomal $VitD_3$'ün hücre proliferasyonunu inhibe etmede serbest formdan daha etkili olduğu ve DOX'un terapötik potansiyelinin $VitD_3$ varlığında arttığı görülmüştür. Optimize edilmiş konsantrasyonlarda $VitD_3$ yüklü FUC kaplı lipozomlar, FUC kaplamalı ve FUC kaplamasız DOX yüklü lipozomlarla karşılaştırılabilir bir etkiye sahiptir. Sonuç olarak, $VitD_3$ ve DOX yüklü ve FUC kaplı lipozomların kanser tedavisinde kombine tedavi olarak uygulanabileceğini düşündürmektedir.

TABLE OF CONTENTS

LIST OF FIGURES ix

LIST OF TABLES xii

CHAPTER 1. INTRODUCTION 1

CHAPTER 2. LITERATURE REVIEW 5

2.1. Vitamin D and Corona Virus 5

2.2. Vitamin D Benefits 6

2.3. Deficiency and Adequate Intake of Vitamin D 6

2.4. Supplementation and Forms of Vitamin D 7

2.5. Vitamin D Synthesis Mechanism 8

2.6. Encapsulation of Vitamin D 9

2.7. Effect of $VitD_3$ on Breast Cancer 11

2.8. Fucoidan 13

2.9. Doxorubicin 15

2.10. Breast Cancer 17

CHAPTER 3. MATERIALS AND METHODS 20

3.1. Materials 20

3.2. Methods 20

3.2.1. Liposome Production 20

3.2.2. $VitD_3$ Loaded Liposome Production 21

3.2.3. UV-Vis Spectrophotometer 22

3.2.4. Effect of EtOH-PBS Mixture on UV Absorbance of $VitD_3$ 23

3.2.5. Temperature Stability of $VitD_3$ 24

3.2.6. Determining Effect of Lipid Concentration on $VitD_3$ 24

3.2.7. Doxorubicin Loaded Liposome Production 25

3.2.8. Size and Zeta Potential Measurements of Liposomes 26

3.2.9. Stability Control of Loaded Liposomes at Body Temperature 29
3.2.10. Determination of the Optimum Centrifugation Time for Liposomes 29
3.2.11. Evaluation of $VitD_3$ Distribution Upon Centrifugation 29
3.2.12. Effect of Cholesterol and $VitD_3$ on Liposome Production..... 30
3.2.13. Encapsulation Efficiency..... 31
3.2.14. Fucoidan Coating on Liposomes..... 32
3.2.15. Fucoidan Coating of Loaded Liposome 32
3.2.16. $VitD_3$ Pretreatment on MDA-MB-231 Cells..... 33
3.2.17. DOX and $VitD_3$ Treatment on MDA-MB-231 Cells 35
3.2.18. Fucoidan Coated and Uncoated $VitD_3$ Loaded Liposome Treatment on MDA-MB-231 Cells..... 36
CHAPTER 4. RESULTS AND DISCUSSIONS 37
4.1. Liposome Production and $VitD_3$ Loading..... 37
4.2. Size and Zeta Potential Measurements of Unloaded Liposomes..... 37
4.3. Size and Zeta Potential Measurements of Loaded Liposomes 38
4.4. Temperature Stability of Liposomes..... 39
4.5. Quantification of $VitD_3$ Using UV-Vis Spectrophotometry..... 42
4.6. Temperature Stability of $VitD_3$..... 42
4.7. Effect of Lipid Concentration on $VitD_3$ Absorbance 43
4.8. Separation of Unloaded $VitD_3$ by Centrifugation..... 47
4.9. Liposomes Loaded with Cholesterol and $VitD_3$ 49
4.10. Encapsulation Efficiency of Liposomes for $VitD_3$ 50
4.11. Fucoidan Coating on Liposomes 51
4.12. $VitD_3$ Pretreatment on MDA-MB-231 Cells 54
4.13. Effect of Fucoidan Coated and $VitD_3$ Loaded Liposomes on Cell Viability 56

CHAPTER 5. CONCLUSIONS 58

REFERENCES 60

LIST OF FIGURES

Figure **Page**

Figure 2.1. Chemical structure of VitD derivatives (Source: Glowka et al., 2019) 8
Figure 2.2. Vitamin D Mechanism (Source: A et al., 2021) 9
Figure 2.3. Structure of a liposome 11
Figure 2.4. Fucoidan structure 13
Figure 2.5. Medical applications of fucoidan (Source: Apostolova et al., 2020) 14
Figure 2.6. Cancer spreading mechanism 1) A leak on the endothelium 2) Malignant cell surrounded by platelets and escape from T-lymphocytes 3) Cancer spreads to the healthy cells. 15
Figure 2.7. Doxorubicin (Source: Carvalho et al., 2009) 16
Figure 2.8.DOX mechanism 1) Simple diffusion of DOX through cell 2) DOX-proteasome complex 3) DOX interferes to the DNA replication/transcription (Source: Carvalho et al., 2009) 16
Figure 2.9.Breast cancer initiation and progression A) Cancer stem cell theory B) Stochastic theory (ER: Estrogen receptor, PR: Progesterone receptor) (Source: Sun et al., 2017) 18
Figure 3.1. (a) Liposome production with passive $VitD_3$ loading. (b) Extruder parts (Source: Avanti Polar Lipids) 22
Figure 3.2. UV-Vis spectrometer principle 23
Figure 3.3. DOX loaded liposome production process. 25
Figure 3.4. Dynamic Light Scattering (DLS) setup 26
Figure 3.5. DLS mechanism (a) Brownian motion of the particles (b) Autocorrelation 27
Figure 3.6. Zeta potential illustration of a negatively charged liposome. 28
Figure 3.7. $VitD_3$ and DOX loaded bare and FUC coated liposome preparation setting 33
Figure 3.8. a) Pellet after centrifugation, b) Cell control, c) Cell culture in flask, d) Thoma Lam for cell counting. 34
Figure 3.9. a) $VitD_3$ added cells on 96-Well plate for 24 hours of observation, b) MTT assay, c) DMSO added well-plate for ELISA. 35
Figure 4.1. $VitD_3$ loaded liposome. 37

Figure **Page**

Figure 4.2. Average size and zeta potential of unloaded and different DSTAP mole percentage involved liposomes in 400 µl PBS + 590 µl ultrapure water. 38
Figure 4.3. Average size and zeta potential measurement of $VitD_3$ loaded liposomes with 15 moles % DSTAP in 400 µl PBS + 590 µl ultrapure water (UPW). 39
Figure 4.4. Average size and zeta potential measurements of unloaded liposomes at different temperatures (a-b) 4 °C (c-d) 25 °C (e-f) 37 °C (Note: all size and zeta potential measurements were done in 400 µl PBS + 590 µl ultrapurte water) 40
Figure 4.5. Effect of temperature on size and zeta potential of liposomes containing 20 moles% of DSTAP as an example 41
Figure 4.6. Average size and zeta potential measurements of 0.25 mg $VitD_3$ loaded (10000 IU) liposome at 37 °C (1 IU = 0.025 µg) 41
Figure 4.7. UV spectrum of $VitD_3$ and other components with liposomes. 42
Figure 4.8. Temperature Stability of $VitD_3$ at 65 °C 43
Figure 4.9. Effect of liposome mixture concentration on $VitD_3$ absorbance in ethanol. 43
Figure 4.10. UV spectra of PBS-EtOH mixtures at different mole fractions of Ethanol, (a) not contained $VitD_3$ (b) contained same amount of $VitD_3$ (c) UV spectra $VitD_3$ obtained by subtracting these two, and Absorbance of PBS-EtOH stock solutions at 265 nm (d) background (e) absorbance of $VitD_3$ after excluding the corresponding background (f) Absorbance of $VitD_3$ at different concentrations estimated by subtracting corresponding background absorbance at the wavelength of 265. Reference cell contained pure ethanol in all measurements. 45
Figure 4.11. Calibration curves of $VitD_3$ in different PBS-Ethanol mixtures at 265 nm. 46
Figure 4.12. Calibration curves of $VitD_3$ in pure ethanol and in a mixture of PBS-Ethanol at 265 nm 46
Figure 4.13. Pellet (at the bottom) and supernatant (at the top) after centrifugation. 47
Figure 4.14. Pellet and supernatant absorbance measurements after centrifugation in ethanol 48
Figure 4.15. Distribution behavior of $VitD_3$ between the pellet and the supernatant upon centrifugation of the liposomes 48

Figure **Page**

Figure 4.16. $VitD_3$ vs Cholesterol spectrum in ethanol and their molecular structure ... 49
Figure 4.17. Encapsulation efficiency of $VitD_3$ loaded liposomes. ... 51
Figure 4.18. Sequential addition of fucoidan to (a) PBS buffer solution, (b) bare liposomes, (c) liposomes containing 10mole% DSTAP. FUC additions were done by 30-minute time intervals. ... 52
Figure 4.19. Effect of fucoidan on (a) zeta potential and (b) size of liposomes at different DSTAP mole%. ... 53
Figure 4.20. Phase separations of FUC added liposomes after 24 hours of storage at 4 °C. ... 54
Figure 4.21. Cell viability of $VitD_3$ treated MDA-MB-231 cells in 24-, 48-, and 72 hours. ... 55
Figure 4.22. Cell viability of DOX and $VitD_3$ treated MDA-MB-231 cells. ... 56
Figure 4.23. Effect of liposomal $VitD_3$ on cell viability (a) only $VitD_3$ loaded liposomes, (b) FUC coated $VitD_3$ liposomes. Also, effect of DOX loaded, and DOX loaded fucoidan coated liposomes were shown. ... 57

LIST OF TABLES

Table **Page**

Table 2.1. Deaths caused by COVID-19 (8th April 2020) (Source: Ilie et al., 2020) 5

Table 2.2. Serum 25-hydroxyvitamin D levels vs health implications (Source: Grant & Holick, 2005) 7

Table 2.3. Nanocarriers for encapsulation of VitD (Source: Ramalho et al., 2017)..... 10

Table 3.1. Amounts of $VitD_3$ used in liposomes composed of DSPC, cholesterol and DSTAP at molar ratio of 65:30:5 (total mole of lipids is 15 μmol)..... 30

Table 3.2. Amounts of cholesterol used in the liposomes composed of DSPC, DSTAP at molar ratio of 65:5 (total mole of lipids is 15 μmol) and containing constant amount of $VitD_3$ (0.28 mg)..... 31

Table 4.1. EtOH mole fraction and the corresponding volumes of PBS and Ethanol (on 10 ml basis)..... 44

CHAPTER 1

INTRODUCTION

Since 2019, the world is suffering from COVID-19 and deaths are continuing because of severe atypical pneumonia. Vitamin D (VitD) is gained attention during pandemic because of its strengthening effect on the immune system. Nevertheless, it has no proven effect on COVID-19 but, there are studies that VitD behaved like a protective agent against viral infections.

Cholecalciferol ($VitD_3$) is the passive form of VitD and can be converted into its active form calcitriol inside the body in necessity. $VitD_3$ is much safer to use in experiments since cells contain necessary enzymes to convert it to its active form calcitriol and excessive amounts of the calcitriol can cause hypercalcemia. However, $VitD_3$ is a new study topic and it must be cleared out the interaction of VitD with the unknown risk factors (El-Sharkawy & Malki, 2020).

VitD has countless benefits such as it has a protective effect for bone diseases, muscle weakness, cancers, multiple sclerosis, and type 1 diabetes mellitus. Even in pregnancy VitD consumption is necessary for fetal bone development and during youth for reducing the risk of MS (Grant & Holick, 2005). Also, VitD reduces the cytokine storm produced by innate immune system, which generates pro-inflammatory and anti-inflammatory cytokines against bacterial infections like COVID-19 (Grant et al., 2020). According to the studies VitD has a renin controlling effect on blood pressure and, beta-endorphin produces during VitD synthesis to generate feeling of well-being, boosting the immune system, relieving pain, promoting relaxation, wound healing, and cellular differentiation (Baggerly et al., 2015). Calcitriol regulates the calcium and phosphorus homeostasis by supporting the intestinal calcium absorption and strengthening the osteoclast function (Muscogiuri, 2020).

Most of the breast cancer cell line contains VitD receptors (VitDR) and $VitD_3$ has a higher affinity for VitDR rather than its active form calcitriol after binding to the VitD binding protein (DBP) (Buras et al., 1994; Medeiros et al., 2020). Different breast cancer cell lines contain different amount of VitDR(Buras et al., 1994). Also, two types of enzymes are needed for hydroxylation reactions of VitD and these enzymes must be found

inside the breast cancer cell in order to convert $VitD_3$ to calcitriol The enzymes available in the breast cancer cells enable $VitD_3$ convert to active calcitriol through two-step hydroxylation reactions. According to Lopes et al. studies on benign and malignant MDA-MB-231 cells, both enzymes were expressed with different amounts in both cell types (Lopes et al., 2010).

Because of its liposoluble behavior, VitD cannot dissolve completely in aqueous solutions. It is sensitive to oxidation because of its double bonds (Abreu Domingues, 2013; Mohammadi et al., 2014). Liposomal encapsulation provides protection and improvement in molecule's solubility, bioavailability, and stability (Glowka et al., 2019; Mohammadi et al., 2014). Liposomal encapsulation of VitD increases its physiological effectiveness by overcoming the high toxicity and low bioavailability problems for administration (Ramalho et al., 2017). Also, encapsulation also helps VitD avoid "first pass effect" of the liver after absorbed by the intestinal mucosa, which means reduction in the number of molecules before it reaches to the target (Ramalho et al., 2017).

Liposomes are small capsules which are composed of self-assembled phospholipids in an aqueous medium and they have a nontoxic, biocompatible, easily functionalized polar head groups and high encapsulation efficiency characteristics (Gonnet et al., 2010; Ramalho et al., 2017). In this study, VitD was encapsulated into liposomes to increase its bioavailability and stability.

Fucoidan (FUC) has been used in cosmetic, food, and dietary supplements for its countless benefits (Citkowska et al., 2019). FUC, known as a sulfated polysaccharide, is found in brown seaweed cell walls and other marine invertebrates including sea cucumber, egg of the sea urchin and seagrasses (Apostolova et al., 2020; Citkowska et al., 2019; van Weelden et al., 2019). It is widely used in pharmacological area because of its antitumor, antimicrobial, antioxidant, anti-inflammatory, and anticoagulant effects (Apostolova et al., 2020). According to the studies, FUC from *Fucus vesiculosus* has an effective blocking adhesion mechanism on platelets for MDA-MB-231 type breast carcinoma cell and over-sulfated structure of FUC from *Fucus vesiculosus* has an inhibitory effect on angiogenesis for breast cancer cell lines (van Weelden et al., 2019).

P-selectin is a type of receptor that is overexpressed in breast cancer cells, and it helps the cancer cells to adhere on platelets to carry within the body which causes metastasis. FUC has a strong binding affinity to p-selectin as an inhibitory effect for preventing the spread of the disease and provides more precise drug targeting (Citkowska et al., 2019; Goubran et al., 2008; Jafari et al., 2020). This feature of FUC was used in targeted drug delivery by coating liposome with FUC and thus targeting them to p-selectins.

Doxorubicin (DOX) is a type of anthracycline that is isolated from a mutated *Streptomyces peucetius* and considered as the one of the most effective chemotherapeutic agents against early and advanced types of breast cancer. Free form of DOX reaches to the nucleus of the cell by decreasing in number, but liposomes help DOX to reduce its distribution, targeting to the cancer cell and protect it against enzymatic degradation (Patel, 1996; Shafei et al., 2017). During the experiments, DOX encapsulated liposomes were given to the VitD pretreated breast cancer cells and its effectiveness was observed.

Breast cancer is the most seen cancer type in women, and it has numerous different types because of its heterogeneous characteristic and can spread through the body such as brain, bone, etc. Treatment pf cancer depends on the tumor biology and molecular characterization and includes surgery, radiation, and chemotherapy (Matsen & Neumayer, 2013; Patel, 1996). There are two theoretical approaches for investigation of breast cancer initiation and progression: namely cancer stem cell theory and stochastic theory. According to the cancer stem cell theory, after a genetic or an epigenetic mutation, tumor develops from the same stem or transit-amplifying (progenitor) cell. On the other hand, stochastic theory suggests that every tumor type develops from a different stem, progenitor or differentiated cell types after random mutations occur (Al-Hajj et al., 2003; Sun et al., 2017).

The objective of the study was to develop $VitD_3$, and DOX loaded liposomes and investigate the effectiveness of $VitD_3$ on therapeutic potential of DOX on MDA-MB-231 triple negative breast cancer cell line. Liposomes were coated with fucoidan to target the selectins overexpressed on breast cancer cells. Targeted liposomes were expected to accumulate in tumor environment to sustain effective concentration and increase drug intracellular delivery. The study showed that $VitD_3$ inhibits the cell viability and enhances the cancer drug (DOX) effect dose dependently. Also, all different amounts of $VitD_3$

loaded liposomes were affected the cell viability almost the same and effect of FUC coated $VitD_3$ loaded liposomes were lower than the bare liposomes. However, FUC coated and uncoated DOX loaded liposomes were affected the $VitD_3$ pretreated cancer cells almost the same.

CHAPTER 2

LITERATURE REVIEW

2.1. Vitamin D and Corona Virus

Since new corona virus spread through Wuhan, Hubei, China by animal-to-human infection in 2019, the third major worldwide epidemic went on and World Health Organization (WHO) renamed the virus as COVID-19 on February 11, 2020. Deaths continued because of the virus in all over the world and the death cause of the infection usually ensued severe atypical pneumonia (Grant et al., 2020). According to Ilie et al. studies based on various countries, there was a negative correlation between levels of mean vitamin D (VitD) and number of cases of COVID-19/1 M population in each country as shown at Table 2.1. (Ilie et al., 2020).

Table 2.1. Deaths caused by COVID-19 (8th April 2020) (Source: Ilie et al., 2020)

Countries	Vit D(25)HD mean (nmol/L)	Cases of COVID-19/1 M	Deaths caused by COVID-19/1 M
Island	57	4736	18
Norway	65	1123	19
Sweden	73.5	834	68
Finland	67.7	449	7
Denmark	65	933	38
UK	47.4	895	105
Ireland	56.4	1230	48
Netherlands	59.5	1199	131
Belgium	49.3	2019	193
Germany	50.1	1309	25
France	60	1671	167
Switzerland	46	2686	103
Italy	50	2306	292
Spain	42.5	3137	314
Estonia	51	893	18
Czech Republic	62.5	488	9
Slovakia	81.5	125	0.4
Hungary	60.6	93	6
Turkey	51.8	453	10
Portugal	39	1289	37

Especially these days, self-protection is very crucial, and VitD seems one of the most helpful protections against the virus. Despite the ongoing studies, there is no evidence for protective effect of VitD against specifically for Covid-19. However,

previous studies showed that VitD is a protective agent against viral infections because of its strengthening effect on the immune system. Based on its immunological and other effects which are not yet known, there is a consideration about protective effect of VitD against Covid-19.

2.2. Vitamin D Benefits

VitD has been investigated because of its countless benefits such as its protective effect for bone diseases, muscle weakness, cancers, multiple sclerosis, and type 1 diabetes mellitus. VitD consumption is necessary during pregnancy for fetal bone development and during youth for reducing the risk of MS (Grant & Holick, 2005). Also, VitD is necessary for cellular immunity to reduce the cytokine storm produced by innate immune system, which generates pro-inflammatory and anti-inflammatory cytokines against bacterial infections like COVID-19 (Grant et al., 2020).

According to Bischoff-Ferrari's studies, in elderly population, VitD decreases the fall risks by 19%, hip fracture risks by 18% and non-vertebral fracture risks by 20%, depending on the adequate dose intakes which are 700 IU VitD per day for fall prevention, 400 IU VitD per day for fracture prevention (Bischoff-Ferrari, 2009).

VitD has a controlling effect of renin which is an important blood pressure regulator protein (Forrest & Stuhldreher, 2011). Also, during VitD synthesis on skin, beta-endorphin is produced as the result of the ultraviolet light type B (UVB) exposure, which generates a feeling of well-being, boosting the immune system, relieving pain, promoting relaxation, wound healing, and cellular differentiation (Baggerly et al., 2015). Additionally, 1,25-dihydroxyvitamin D regulates the calcium and phosphorus homeostasis by supporting the intestinal calcium absorption and strengthening the osteoclast function (Muscogiuri, 2020).

2.3. Deficiency and Adequate Intake of Vitamin D

VitD deficiency can be seen even in sun-seeing countries because of the sunshine blocking traditional costumes (Mohammadi et al., 2014). Serum 25(OH)D concentrations decrease during aging while case-fatality rates increase. Modern life working schedules and reduced VitD production decrease 7-dehydrocholesterol levels in the skin. Also, some pharmaceutical drugs such as antiepileptics, antineoplastics, antibiotics, anti-

inflammatory agents, antihypertensives, antiretrovirals, endocrine drugs, and some herbal medicines, reduce the serum 25(OH)D concentrations in the blood (Grant et al., 2020).

As shown in Table 2.2, serum concentrations of 25-hydroxyvitamin D below 20 ng/mL (50 nmol/L) is defined as deficiency and people that obese, with poor health status, hypertension, low high-density lipoprotein (HDL) cholesterol level and not consuming dairy products daily have a higher risk than those having daily supplementation. Forrest et al. support the fact that low HDL cholesterol is independently and significantly correlates with VitD deficiency (Forrest & Stuhldreher, 2011). According to the Institute of Medicine (IOM), the recommended adequate intake is 200 IU per day for adults up to 50 years of age, 400 IU per day for adults between age of 51 and 70, and 600 IU per day for those aged 70 years and over (Bischoff-Ferrari, 2009). Magnesium is also recommended with the intakes since it is an important activator for VitD to regulate calcium and phosphate levels to maintain a good bone health (Grant et al., 2020).

Table 2.2. Serum 25-hydroxyvitamin D levels vs health implications (Source: Grant & Holick, 2005)

25(OH)D Level (ng/mL)	25(OH)D Level (nmol/L)	Health Implications
<20	<50	Deficiency
20-32	50-80	Insufficiency
32-100	80-250	Sufficiency
54-90	135-225	Normal in sunny countries
>100	>250	Excess
>150	>325	Intoxication

2.4. Supplementation and Forms of Vitamin D

Cholecalciferol as vitamin D_3 ($VitD_3$) and ergocalciferol as vitamin D_2 ($VitD_2$) are considered the main form of $VitD_3$. Dietary supplements and fortified foods with VitD are available for $VitD_3$ supplementation, and plant originated supplements such as some mushrooms are available products for $VitD_2$ supplementation. $VitD_3$ is the inert form of VitD, and it can convert into calcitriol, its active form, with two hydroxylation processes. Due to its structural similarities with the steroid hormones, calcitriol binds to VitDR and regulates target gene expression via both genomic and nongenomic pathways. Since $VitD_3$'s binding affinity to the receptors is higher than $VitD_2$, it is more potent and much suitable for commercial preparations and food fortifications; but, $VitD_2$ can be considered

as an alternative for vegan and vegetarians (Glowka et al., 2019; Maurya et al., 2020; Ramalho et al., 2017).

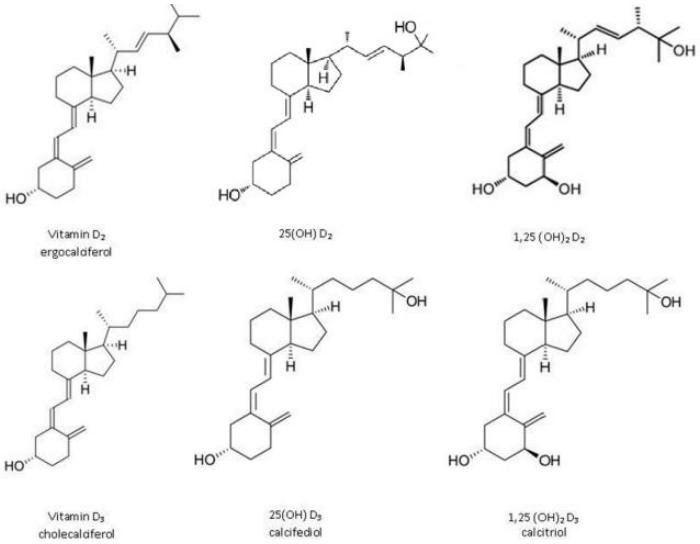

Figure 2.1. Chemical structure of VitD derivatives (Source: Glowka et al., 2019)

2.5. Vitamin D Synthesis Mechanism

VitD synthesis starts in the skin with 290 to 315 nm wavelength ultraviolet (UV) light exposure and the most recommended time interval for VitD synthesis during the day is between 10 AM to 3 PM. In the skin, 7-dehydrochlesterol (7-DHC) converts into pre-vitamin D by the stimulation effect of 290-315 nm UV lights, as pre-vitamin D is thermally isomerized to the inert cholecalciferol ($VitD_3$). Also, VitD can be supplied from food and dietary products such as egg yolk, flesh of fatty fish and fish liver oils, but either way 7-dehydrocholesterol undergoes 2 hydroxylation reactions to transform into the active form calcitriol. During hydroxylation reactions, CYP24A1 and CYP27B1 enzymes help the synthesis of calcitriol. CYP27B1 converts $VitD_3$ (25-hydroxyvitamin D) ($25(OH)D_3$) to active form calcitriol (1,25-dihydroxyvitamin D) ($1,25(OH)_2D_3$), and CYP24A1 plays a negative feedback role for the transcription.

The first hydroxylation reaction takes place in the liver and pre-vitamin D converts into $VitD_3$. Second hydroxylation reaction happens in the kidneys and $VitD_3$ converts into calcitriol. However, once VitD is produced, it does not remain in the blood circulation for a long time; it is stored almost instantly in the adipose tissue or metabolized in the liver (Baggerly et al., 2015; Forrest & Stuhldreher, 2011; Glowka et al., 2019; Ramalho et al., 2017; Umar et al., 2018; Voutsadakis, 2020).

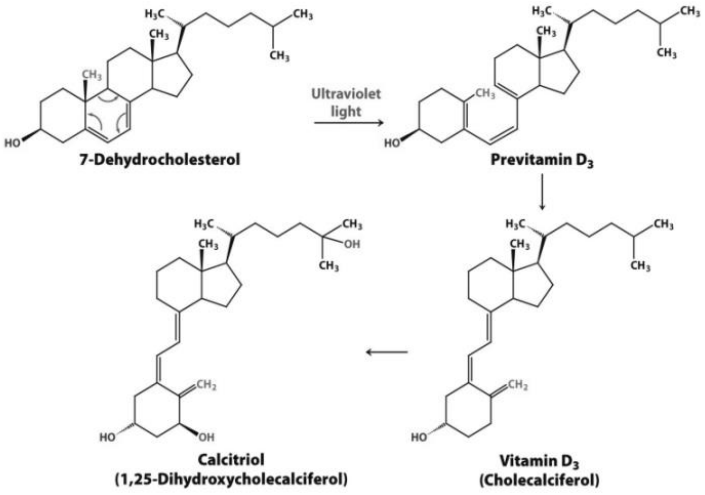

Figure 2.2. Vitamin D Mechanism (Source: A et al., 2021)

VitD absorbs in the small intestine after the oral ingestion, as it is a lipophilic vitamin, and usually carried as $VitD_3$ and calcitriol in the blood with VitD binding protein (DBP) at a rate of 85-87%, albumin at a rate of 12% or unbound at a rate of 1%. $1,25(OH)_2D_3$ regulates intestinal calcium absorption and osteoclast function in order to maintain the calcium-phosphorus homeostasis and bone health. It binds to VitDR, which can be found in most of the internal organs such as kidney, adrenal gland, thyroid gland, bladder, gastrointestinal (GI) tract, liver, prostate, breast cells and normal human colon cells, then, $1,25(OH)_2D_3$-VitDR complex binds to Retinoid X receptor (RXR) and a heterodimer form occurs. To initiate the transcription process, heterodimer form binds with VitD responsive elements (VitDRE) in the promoter region of the target genes. VitDR has co-activators and co-repressors. So, when it binds with the coactivators, the transcription process starts and, when it binds with co-repressors the transcription gets repressed (Kadappan, 2019; Maurya & Aggarwal, 2017; Muscogiuri, 2020).

2.6. Encapsulation of Vitamin D

Encapsulation provides protection and controlled release of desired materials in nano or micro capsules, and it can be used in drug delivery systems (DDS) and food fortification processes (Table 2.3). Physiological behaviors of the materials can get improved by encapsulation, which enables enhanced solubility, bioavailability, and stability of bioactive materials (Glowka et al., 2019; Mohammadi et al., 2014).

$VitD_3$ is a liposoluble vitamin which cannot dissolve completely in aqueous solutions, due to its low polarity characteristic and sensitivity to oxidation because of its

double bonds (Abreu Domingues, 2013; Mohammadi et al., 2014). Also, it has a high toxicity and low bioavailability when it comes to the administration (Ramalho et al., 2017). Encapsulation is a promising technology to overcome these problems by improving VitD's physiological effectiveness. VitD also suffers from "first pass effect" of the liver after absorbed by the intestinal mucosa, which means the deactivation of the VitD. This effect causes the amount of VitD to decrease before it reaches the target organ (Ramalho et al., 2017). Encapsulation can help VitD to carry through its target more effectively.

Table 2.3. Nanocarriers for encapsulation of VitD (Source: Ramalho et al., 2017)

Nanocarrier	Indication	Development phase			Animal studies
		Physicochemical studies	Release studies	Cellular studies	
PLA NPs	Cancer treatment	DLS, EE, stability	PBS	Human breast cancer cells (MCF-7); MTT assay; cellular uptake (Fluorescence microscopy)	n/a
PLGA NPs	Cancer treatment	DLS, ELS, TEM, stability	PBS	Human pancreatic cell lines (S2-013 and hTERT-HPNE); lung cancer cell line (A549); SRB assay, cellular uptake and morphology (confocal microscopy); flow cytometry (cell cycle analysis)	n/a
HAp-PLGA NPs	Osteogenesis and bone tissue differentiation	XRD, FTIR, DLS, ELS	n/a	Mouse calvarial preosteoblastic cell line (MC3T3-E1), confocal microscopy	Rats with osteoporosis and induced bone defects, pathohistological analysis of bone tissue after sample injection
Quantum dots	Cancer diagnosis and treatment	FTIR, AFM	n/a	Mouse myoblast cell line (C2C12), confocal microscopy, luciferase activity assay (gene expression)	n/a

Liposomes can carry both hydrophilic and hydrophobic molecules with their aqueous medium and lipid bilayer. They are basically small capsules composed of self-assembled phospholipids in an aqueous medium and they can be classified according to their number of bilayers and size. As they have nontoxic, biocompatible, easily functionalized polar head groups and high encapsulation efficiency characteristics,

liposomes are usually preferred in nanomedicine applications. On the other hand, they have low solubility, short half-life, high production cost and indecisive stability which depends on both inside and outside interactions. Phospholipid bilayer can get oxidized, and leakage can be a possible for encapsulation of low molecular weight molecules (Gonnet et al., 2010; Ramalho et al., 2017).

Based on the preparation method of liposomes, cholesterol can decrease the vehicle size and the phospholipid bilayer permeability to small hydrophilic solutes and ions. On the other hand, liposomal membrane can get more stable with the presence of cholesterol in biological fluids by increasing the viscosity (Mohammadi et al., 2014).

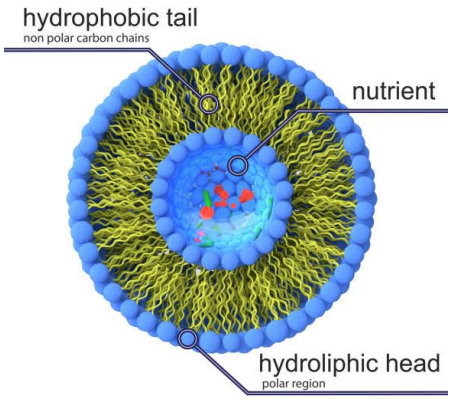

Figure 2.3. Structure of a liposome

2.7. Effect of $VitD_3$ on Breast Cancer

80-90% of the breast cancer cell lines contains VitD receptors (VitDR), and cholecalciferol ($VitD_3$) has a higher affinity for VitDR rather than its active form calcitriol after binding to the VitD binding protein (DBP), which is a very important characteristic for VitD applications (Buras et al., 1994; Medeiros et al., 2020). According to Buras et al., MDA-MB-175 cell line expressed the highest level of VitDR, on the other hand, MDA-MB-231 expressed the lowest level of VitDR receptors. The studies also showed that low receptor levels are associated with the late development of lymph node metastases and number of the receptors are not related with the stage of the cancer (Buras et al., 1994). However, despite the lowest level of VitDR level, another study of Guo et al. showed that VitD (calcitriol) combination with different metformin ratios treatment increased the apoptotic cell number on the MDA-MB-231 breast cancer cell line, indicating the possibility of VitD treatment on MDA-MB-231 cell lines (Guo et al., 2015).

CYP27B1 and CYP24A1 enzymes are necessary for hydroxylation reactions of VitD. These enzymes available in breast cancer cells enable $VitD_3$ to convert to calcitriol through two-step hydroxylation reaction. According to Lopes et al. studies on benign and malignant MDA-MB-231 cells, both enzymes were expressed with different amounts in both cell types. While CYP27B1 expression was higher in benign cells, CYP24A1 expression was higher in carcinoma cells (Lopes et al., 2010).

VitD has been used due to its anti-cancer effect on breast cancer studies for a while. In Sabzichi et al. studies, VitD loaded nanostructured lipid carriers (NLC) were used to enhance the efficacy of doxorubicin (DOX) on breast cancer cells (MCF-7). The results showed that, highest percentage of cell death occurred after DOX treatment with VitD loaded liposomes (Sabzichi et al., 2017). According to Kutlehria et al. study of breast cancer treatment with DOX carrying cholecalciferol-PEG (PEGCCF) conjugate nanomicelles on MCF10A, MDA-MB-468, and MDA-MB-231 cell lines, highest cytotoxycity and lowest cell migration levels were observed after application of DOX and $VitD_3$ together on the cell lines. PEGCCF conjugated nanomicelles helped for a more sustained DOX release and efficacy of DOX increased after encapsulated inside the nanomicelles (Kutlehria et al., 2018). In another study, Zheng et al. showed that VitDRs induced with VitD increased the tamoxifen sensitivity in MCF-7 stem cells and suppressed the Wnt/β-catenin signaling path. Wnt/β-catenin signaling pathway promotes tumor and metastasis formation and stimulates them to reach targeted genes. In the study, it was observed a dose dependent rise in the apoptotic cell percentage and reduction in the proliferation ability on VitD treated cells. When $CD133^{+/-}$ stem cells of MCF-7 were examined, VitDR expression was found higher in $CD133^-$ and as a consequence of that, Wnt/β-catenin protein expression was lesser than $CD133^+$ and Wnt/β-catenin signaling pathway got interrupted by VitDR on $CD133^-$ stem cells. It was considered that the tamoxifen resistance of $CD133^+$ stem cells were high because of low expression levels of VitDR (Zheng et al., 2018).

$VitD_3$ is considered as a much safer molecule rather than calcitriol because it can be converted into calcitriol inside the body as much as the need and excessive amount of calcitriol can cause hypercalcemia. According to Healthy et al. studies on different mammary gland cancer bearing mice with supplementation or deficiency of VitD indicated that $VitD_3$ and calcitriol (VitD) amounts affect differently depending on the stage of the tumor development (Healthy et al., 2020). The role of VitDR among different

types of breast tumors (El-Sharkawy & Malki, 2020) has not been known yet; therefore, it remains as a study still to be investigated.

2.8. Fucoidan

Since fucoidan (FUC) discovered by Kylin in 1913 (Kylin, 1913), it has been widely used in many experimental research areas because of its biological features. Although there are no registered drug products that include fucoidan yet, it has been used in cosmetic, food, and dietary supplements area for its countless benefits (Citkowska et al., 2019).

Fucoidan is known as a sulfated polysaccharide and found in brown seaweed cell walls and other marine invertebrates including sea cucumber, egg of the sea urchin and seagrasses. Although the chemical composition and molecular weight of fucoidan can vary depending on the extraction process, growth environment, geographic location, and season, the backbone of fucoidan is always made up of a repeating pattern of α-(1→3) linked α-l-fucose or alternating α-(1→3) and α-(1→4) linked α-l-fucose residues (Fig. 2.4). There are many sulfate groups located on C-2, C-3 and C-4 positions that gives the negative charge of the molecule, and an increase in sulfate group means increase in the negative charge which causes a stronger bioactivity (Apostolova et al., 2020; Citkowska et al., 2019; van Weelden et al., 2019).

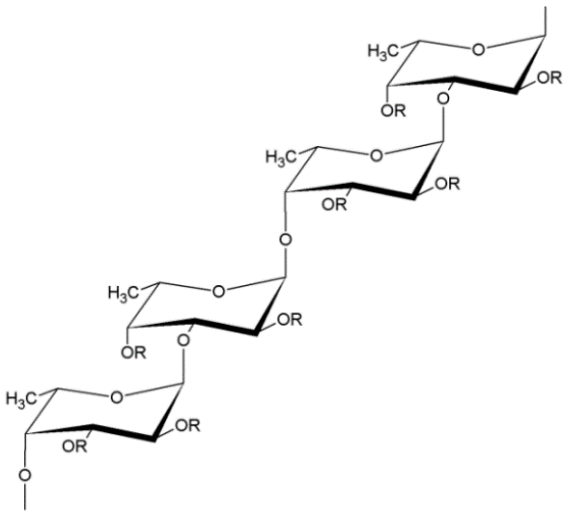

Figure 2.4. Fucoidan structure

Fucoidan has been investigated because of its numerous benefits such as antitumor, antimicrobial, antioxidant, anti-inflammatory, and anticoagulant effects especially in pharmacological area (Apostolova et al., 2020).

Figure 2.5. Medical applications of fucoidan (Source: Apostolova et al., 2020)

Studies showed that fucoidan from *Fucus vesiculosus* has an effective blocking adhesion mechanism on platelets for MDA-MB-231 type breast carcinoma cell, which is a crucial feature for preventing the cancer cells to spread within the body (metastasis). Also, it has been reported that fucoidan from *Fucus vesiculosus* has an inhibitory effect on hydroxyl and superoxide radical formation. Hydroxyl radicals attack the cell membrane inside the body and damage the sugar groups and sequences of DNA bases, which causes a decomposition on double-helix structure to lead cell death or mutation (Li et al., 2008). Moreover, the over-sulfated structure of fucoidan from *Fucus vesiculosus* has an inhibitory effect on angiogenesis for breast cancer cell lines. The anti-proliferative effect increases while sulfate group numbers on the backbone of fucoidan increase. In addition, in hormone dependent cancers such as breast cancer, fucoidan from *Fucus vesiculosus* has a blocking effect on estrogen pathway which causes a proliferative effect on carcinoma cells (van Weelden et al., 2019).

Fucoidan interacts with P-selectin. P-selectin is a type of receptor that is overexpressed on breast cancer cells such as MDA-MB-231, but not on normal cell tissue. It helps the cancer cells to adhere on platelets to carry within the body which causes metastasis. During the leak on an endothelium, p-selectin binds with platelets and forms a cluster of major histocompatibility complex class I (MHC-I) by surrounding the carcinoma cell to escape from the T-cell mediated immunity, which is the natural killer of the body against foreign molecules. Since T-lymphocytes could not recognize tumor MHC-I by their tumor MHC-I receptor, the cluster reaches the healthy tissues. According to the studies, fucoidan has a strong binding affinity to p-selectin as an inhibitory effect

for preventing the spread of the disease and provides more precise drug targeting. It has a natural ligand characteristic for p-selectins and can bind covalently to receptor (Citkowska et al., 2019; Goubran et al., 2008; Jafari et al., 2020; Novoyatleva et al., 2019).

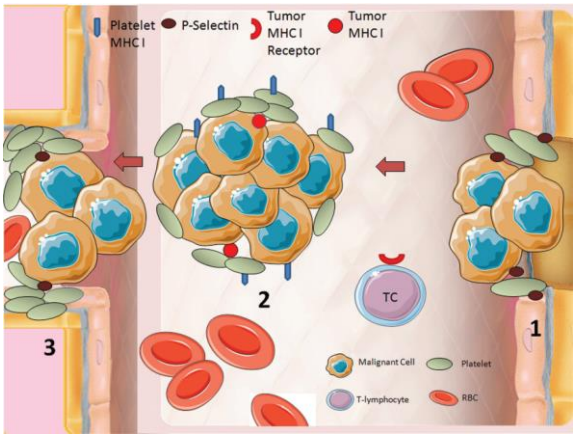

Figure 2.6. Cancer spreading mechanism 1) A leak on the endothelium 2) Malignant cells surrounded by platelets and escape from T-lymphocytes 3) Cancer spreads to the healthy cells.

In this study, fucoidan was used for coating of liposomes to promote targeted drug delivery. The most important issue for drug targeting studies is to protect the healthy tissues while trying to exterminate the carcinoma cells. By using the strong binding affinity of fucoidan to p-selectin, $VitD_3$ loaded fucoidan coated liposomes was considered to target directly to the carcinoma cells while protecting the healthy cells against contamination from cancer drug. Consequently, it is expected that enough doses of drug could be delivered to the carcinoma cells using less dose of the drug.

2.9. Doxorubicin

Doxorubicin (DOX), also known as Adriamycin® or Doxil®, is one of the first found anthracyclines that isolated from a mutated *Streptomyces peucetius* in 1960s, which is a type of an antibiotic. Because of the multiple side-effects of anthracyclines, such as cardiotoxicity, acute nausea and vomiting, there are ongoing studies for its chemical modification and substitution so that more than 200 analogs have been produced in an effort for finding a less toxic anthracycline.

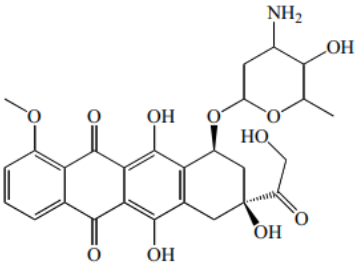

Figure 2.7. Doxorubicin (Source: Carvalho et al., 2009)

DOX is considered as the one of the most effective chemotherapeutic agents against early and advanced types of breast cancer. However, due to its side-effects, there are some dosage limitations for usage on patients such as 400-700 mg/m^2 in adults and 300 mg/m^2 in children mentioned as threshold levels. DOX enters the nucleus and interferes to the DNA replication/transcription and cause cell death. Because of this reason DOX also referred as topoisomerase II poison in some studies since topoisomerase II catalysis the unwinding of the DNA without causing any change (Carvalho et al., 2009; Renu et al., 2018; Shafei et al., 2017).

When DOX is administered as free form, only its small amount reaches the nucleus of the cell. Therefore, high doses of DOX need to be administered to increase its concentration at the site of interest. Liposomes help DOX to reduce its biodistribution and accumulate in the cancerous tissues. Liposomes are small molecules that can pass through the leaky endothelial of cancerous tissues and help to increase the therapeutic index of the drug. Moreover, by covering with a phospholipid barrier, DOX becomes protected against enzymatic degradation (Patel, 1996; Shafei et al., 2017).

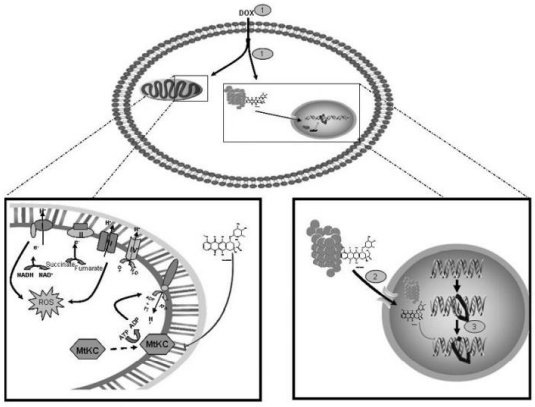

Figure 2.8. DOX mechanism 1) Simple diffusion of DOX through cell 2) DOX proteasome complex 3) DOX interferes to the DNA replication/transcription (Source: Carvalho et al., 2009)

DOX enters the cell by using simple diffusion and binds to 20S proteasomal subunit to form a DOX-proteasome complex in the cytoplasm. It carries to the nucleus with this complex and binds to DNA with higher affinity. Also, DOX can bind with mitochondria and blocks the mitochondrial creatine kinase (MtCK) to bind with cardiolipin, which is a lipoprotein located in the inner membrane of the mitochondria. These reactions cause an increase in reactive oxygen species (ROS) (Carvalho et al., 2009).

2.10. Breast Cancer

Breast cancer is known as the most common cancer type seen in 26% of women (Shafei et al., 2017). It has numerous different types because of its heterogeneous characteristic and can spread through the body such as brain, bone, etc. When a cancer has a tendency to spread, it is called as metastatic breast cancer (MBC) and after the spread, survival rate of patients is known to be about 2-3 years (Patel, 1996; Sun et al., 2017).

According to the Turk Cancer Society, women at the age between 20-40 should take an ultrasound and clinical breast examination control once in two years and women after 40 years old should take a mammography once in two years (https://www.turkkanserdernegi.org). If the suspicious abnormality gets confirmed as tumor tissue, treatment depends on the tumor biology and molecular characterization. Treatment includes surgery, radiation, and chemotherapy. Chemotherapy is offered for tumor size bigger than 2 cm and anthracycline (such as doxorubicin) treatment is administered. Radiation therapy is offered for tumor size bigger than 5 cm or tumors for close margins to risky organs (Matsen & Neumayer, 2013; Patel, 1996).

Breast cancer is generally seen as ductal hyperproliferation that grows into benign tumor or MBC by numerous carcinogenic factors. According to the studies on normal and tumor cells, non-identical DNA methylation patterns observed that explain carcinogenesis can be developed upon epigenetic mutations in the microenvironment. Cancer stem cells (CSCs) have been investigated as newly discovered malignant cells which are related with tumor initiation, recurrence, and escape. They can evolve from normal tissues into stem or progenitor cells and have a self-renewal and resistance to chemotherapy and radiotherapy potential. Breast cancer stem cells (bCSCs) can develop a tumor with 100 cells. Nowadays cancer stem cell theory and stochastic theory have been

developed for explaining breast cancer initiation and progression. According to the cancer stem cell theory, after a genetic or an epigenetic mutation, tumor develops from the same stem or transit-amplifying (progenitor) cell. On the other hand, stochastic theory suggests that every tumor type develops from a different stem, progenitor or differentiated cell types after random mutations occur (Al-Hajj et al., 2003; Sun et al., 2017).

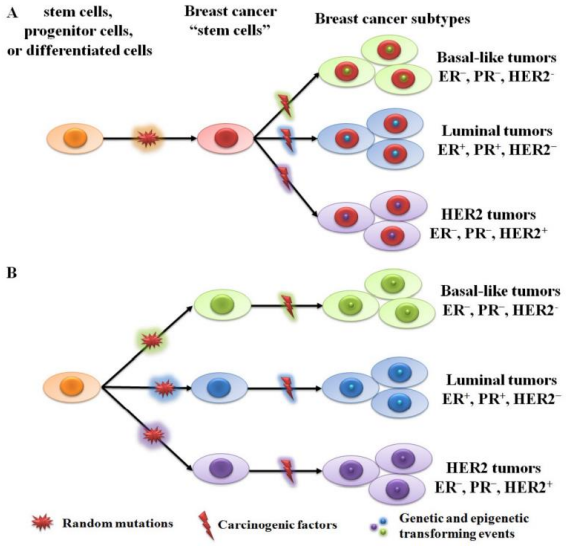

Figure 2.9. Breast cancer initiation and progression A) Cancer stem cell theory B) Stochastic theory (ER: receptor, PR: Progesterone receptor) (Source: Sun et al., 2017)

Related Genes can be summarized as follows: BRCA 1 and 2 genes were discovered in 1994, and they give an insight information about breast cancer biology. They are both lifetime risk factors with 60% and 80% percent changes respectively and have a potential to develop malignant neoplasm such as ovarian, pancreatic, and male breast cancer. In the cell, BRCA1 expression repression causes centrosome duplication abnormality, genetic instability, and apoptosis. BRCA2 takes place in the DNA double-strand repairs and a mutation in BRCA2 usually develops an invasive ductal carcinoma (Matsen & Neumayer, 2013; Sun et al., 2017).

Human epidermal growth receptor (HER2) normally takes place in gene amplification and re-arrangement. However, it was observed that normal mammary duct formation gets damage in HER2 genes taken mouse model and in the case of overexpression as seen in primary breast cancer with 20%, number of the breast cancer stem cells gets increase (Sun et al., 2017).

Epidermal growth factor receptor (EGFR) is normally responsible for cell proliferation promotion, cell invasion, angiogenesis, and apoptosis prevention in the cell. On the other hand, a mutation in the receptor can cause overexpression and lead inflammatory breast cancer with 30% rate (Sun et al., 2017).

c-Myc takes place as a transcription factor and according to the genome-wide screening, it controls 15% of all the genes. Usually, in high-graded invasive breast carcinoma cells, c-Myc is overexpressed and in benign tissues, c-Myc not found (Sun et al., 2017).

MDA-MB-231 cell line is a triple-negative breast cancer (TNBC) cell line that is very aggressive, invasive, and not completely differentiated. It is called “basal” human breast cancer cell line since it does not contain any estrogen receptor (ER), progesterone receptor (PR) or HER2 amplification. MDA-MB-231 cell line, which is an epithelial, was reproduced from a metastatic mammary adenocarcinoma diagnosed 51-year-old female and it has been widely used for medical research (Ecacc, 2022; Media, 2014).

CHAPTER 3

MATERIALS AND METHODS

3.1. Materials

Cholecalciferol ($VitD_3$) (7-dehydrocholesterol), cholesterol, sodium chloride (NaCl), sodium phosphate monobasic dihydrate ($NaH_2PO_4.2H_2O$), sodium phosphate dibasic dihydrate ($Na_2HPO_4.2H_2O$), for PBS buffer preparation, were purchased from Sigma-Aldrich, Inc. (St. Louis, MO, USA). 1,2-stearoyl-3-trimethylammonium-propane (chloride salt) (DSTAP), 1,2-distearoyl-sn-glycero-3-phosphocholine (DSPC), filter supports (Avanti Number: 610014), and Nuclepore Track-Etch Membrane (Whatman) for extrusion were purchased from Avanti Polar Lipids Inc. (Alabaster, AL, USA).

3.2. Methods

3.2.1. Liposome Production

Liposomes were prepared by thin-film hydration method using phosphate-buffered saline (PBS). In preparation of liposomes, 1,2-distearoyl-sn-glycero-3-phosphocholine (DSPC) was used as the main lipid, and 1,2-stearoyl-3-trimethylammonium-propane chloride salt (DSTAP) was used to obtain positively charged cationic liposomes for negatively charged fucoidan coating. Liposomes were designed by keeping cholesterol molar percent constant at 30% and varying DSPC and DSTAP molar percentages accordingly while keeping the total lipid amount as 15 μmol. Figure 3.1(a) shows the steps of making liposomes. Predetermined amounts of DSPC, cholesterol and DSTAP were weighted into a scintillation vial and the 2 ml of chloroform was added to homogenize the mixture. The vial was put on a shaker to completely dissolve the liposome mixture. Chloroform was removed by purging the solution on the shaker with nitrogen gas stream. The vial was put in a vacuum oven (Nüve EV 018) overnight at room temperature for complete removal of chloroform, resulting in a thin-film on the vial surface. To the resulting thin film, 1 ml of PBS was added and put in the water bath at 65 °C for 1 hour for hydration.

For preparation of PBS (150 mM, pH=7.2), 0.0600677 g sodium phosphate monobasic dihydrate ($NaH_2PO_4.2H_2O$), 0.120588225 g sodium phosphate dibasic dihydrate ($Na_2HPO_4.2H_2O$) and 2.26706292 g sodium chloride (NaCl) were weighted and transferred to a volumetric flask. After 250 ml ultra-pure water (UPW) addition, the flask was put on a magnetic stirrer for 10 minutes. pH of the solution was adjusted to 7.2 by 1M of sodium hydroxide (NaOH) solution.

After the hydration of the thin-film, liposomes were produced using mini extruder (Avanti Mini Extruder). The extruder consists of an outer casing and a retainer nut that keeps together the internal membrane supporting a Teflon bearing (Figure 3.1(b)). Between the internal membrane supports, a 200 nm pore sized polycarbonate membrane (Whatman Nuclepore Track-Etch Membrane Filtration Products) and filter supports (Avanti Number: 610014 Filter Supports 100 / Pack) squeezed while the solution was passed through the pores and force lipids to came together and form liposomes.

The extruder was placed on its holder preheated to 65 °C on a hot plate to ensure that the lipids were above their phase transition temperature. Two Hamilton syringes, one filled with the PBS solution and the other one empty, were connected to both sides of the extruder and PBS solution was passed through only one time to fill the empty parts between the filter supports and membrane. Then, hydrated pre-liposome solution was taken from the vial to Hamilton syringe and attached to the extruder. Solution was passed through the extruder 11 times to form liposomes by using a syringe pump (LongerPump LSP04-1A) to push the plunger of the Hamilton syringe at constant flow rate of 120 mm/min. After the extrusion, liposome solution was transferred into an opaque vial and stored in the fridge at 4 °C until further use.

3.2.2. $VitD_3$ Loaded Liposome Production

$VitD_3$ loaded liposomes were prepared with passive loading. Cholecalciferol ($VitD_3$) is an oil-soluble molecule. Predetermined amount of $VitD_3$ was added to the liposome mixture during thin-film preparation in a brown vial because $VitD_3$ is light-sensitive. 0.025 μg $VitD_3$ corresponds to 1 international unit (IU), and all $VitD_3$ loadings were done by this proportion during experiments. Since $VitD_3$ can dissolve in both ethanol and chloroform, homogenization of lipids with $VitD_3$ was done either in ethanol or chloroform (Liang et al., 2012).

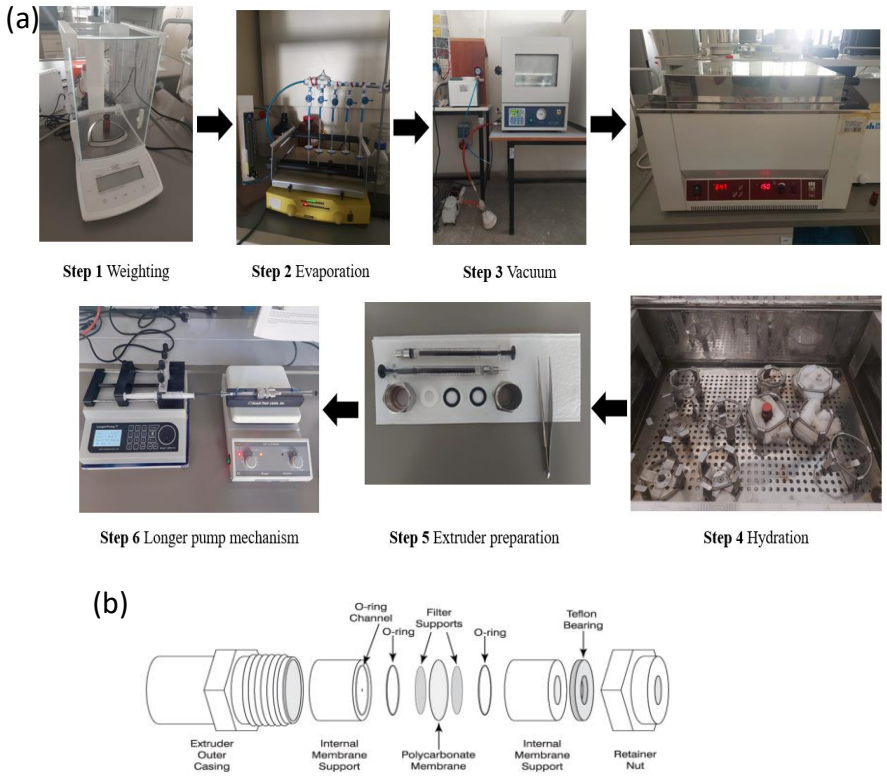

Figure 3.1. (a) Liposome production with passive $VitD_3$ loading. (b) Extruder parts (Source: Avanti Polar Lipids)

3.2.3. UV-Vis Spectrophotometer

UV-vis spectrophotometry (Perkin Elmer Lambda 25) was used to determine the amount of cholecalciferol loaded into liposomes (Dalmoro et al., 2019). Light absorption measurements were done by UV-Vis spectrometer by applying Bouguer-Lambert-Beer law (Eq. 3.1).

$$\lg\left(\frac{I_0}{I}\right)_{\tilde{\nu}} = \lg\left(\frac{100}{T(\%)}\right)_{\tilde{\nu}} \equiv A_{\tilde{\nu}} = \varepsilon_{\tilde{\nu}} \cdot c \cdot d \qquad (3.1)$$

where $A_{\tilde{\nu}} = \lg\left(\frac{I_0}{I}\right)_{\tilde{\nu}}$ means absorbance, $T_{\tilde{\nu}} = \frac{I}{I_0} \cdot 100$ means transmittance, ε_v means the molar extinction coefficient and I_0 represents the entering light intensity to the sample. I represent the coming up light intensity through the sample. c is the concentration of the light-absorbing sample and d means the length of the path. ε_v depends on the wavenumber (v) or wavelength (λ). There is a correlation between ε_v and v that gives the absorption

spectrum. ε_v can be changed in the samples' absorption spectrum and logarithmic value of log ε = f(v) is used for determining the absorption spectrum (Figure 3.2) (Perkampus, 1992).

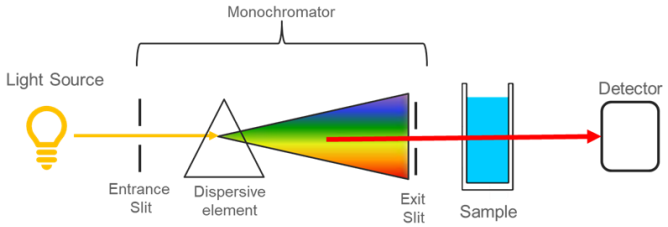

Figure 3.2. UV-Vis spectrometer principle

UV absorbance of cholecalciferol was measured in ethanol since it has very high solubility in ethanol (50 mg/ml, Sigma-Aldrich Inc.). Cholecalciferol ($VitD_3$) was dissolved in ethanol and spectrum was taken in the full scan of the wavelength to determine the maximum absorbance wavelength. To ensure no interference from other components in the solution, full spectrums of liposomes mixed with ethanol and water as well as ultra-pure water were obtained. After determination of maximum absorbance wavelength, calibration curve of $VitD_3$ was produced by dissolving the known amount of $VitD_3$ in ethanol and performing serial dilution.

3.2.4. Effect of EtOH-PBS Mixture on UV Absorbance of $VitD_3$

In order to investigate the effect of EtOH-PBS mixtures on UV absorbance of $VitD_3$, a separate experiment was designed. 1.26 mg $VitD_3$ was dissolved in 2 ml ethanol, resulting in 0.63 mg/ml stock solution. Then, 11 different vials were prepared containing different volumes of PBS solution. Ethanol was added to complete a final volume of 10 ml. Therefore, Different ethanol mole fractions (y_{EtOH}) were obtained calculated according to Eq. 3.2.

$$y_{EtOH} = n_{EtOH} / (n_{EtOH} + n_{PBS}) \quad (3.2)$$

where y is mole fraction and n are number of moles. A stock solution of $VitD_3$ was prepared in pure EtOH. 100 µl of $VitD_3$ stock solution was putted in an opaque vial and 2 ml of 1st PBS + EtOH stock solution added on it. A serial 1:1 dilution was done up to 6 vials to obtain different $VitD_3$ concentrations using the same PBS + EtOH stock solution. The same dilutions were carried on for the other PBS + EtOH stock solution at different y_{EtOH} mole fractions. Also, these different dilutions were used as calibration curves. Absorbance of each vial were measured at 265 nm and full spectrum scan (btw. 200-800

nm) were obtained for each PBS + EtOH stock solution by the UV-Vis Spectrometer (Perkin Elmer Lambda 25).

For crosscheck of the results, another $VitD_3$ in PBS + EtOH experiment was designed. First, 0.1 mg/ml $VitD_3$ stock solution was prepared and aliquoted as 100 µl into 12 different Eppendorf tubes. Then, 0-2-5-10-20-30-50-80-90-100-120-150 µl PBS was added into the tubes respectively. Each tube was completed to final volume of 1000 µl with EtOH, and their absorbance was measured with UV-Vis Spectrometer (Perkin Elmer Lambda 25). For the background absorbances, 0-2-5-10-20-30-50-80-90-100-120-150-170-190-220-250-280-300 µl PBS was added into the 18 different Eppendorf tubes and tubes was completed to final volume of 1000 µl with EtOH. Their absorbance was measured by UV-Vis Spectrometer (Perkin Elmer Lambda 25).

3.2.5. Temperature Stability of $VitD_3$

As mentioned above, for production of $VitD_3$ loaded liposomes, thin-film is hydrated at 65 °C. To control the stability of cholecalciferol ($VitD_3$) during hydration process of liposome production, 0.5 mg $VitD_3$ was dissolved in 5 ml ethanol in an opaque brown vial, resulting in 0.1 mg/ml stock solution. Then, the vial was put in a water bath at 65 °C. 100 µl of the solution was withdrawn from the vial by piercing the lid with a glass syringe at every 15 minutes for 2 hours. Each sample was diluted by adding 500 µL ethanol and their absorbance values were measured by UV-Vis Spectrometer (Perkin Elmer Lambda 25) at 265 nm, which is the maximum absorbance wavelength of $VitD_3$ in ethanol.

3.2.6. Determining Effect of Lipid Concentration on $VitD_3$

The effect of DSPC, cholesterol and DSTAP lipid concentration on absorbance of cholecalciferol ($VitD_3$) was examined. 0.1 mg/ml $VitD_3$ stock solution was prepared and aliquoted into Eppendorf tubes as 20 µl. In a liposome formulation with 15% DSTAP (2.25 mg), 30% cholesterol (2.48 mg) and 55% DSPC (9.3 mg), total mass of lipids was approximately 14.05 mg, to which 140.5 µl of ethanol was added to get 0.1 mg/ml final concentration. Lipid solution was added on the $VitD_3$ contained Eppendorf tubes at increasing amounts. Ethanol was added into each tube till all of them reached to a final volume of 600 µl. Tubes were mixed with a shaker and their absorbance values were measured at 265 nm.

3.2.7. Doxorubicin Loaded Liposome Production

For doxorubicin (DOX) loaded liposomes, lipids of DSPC, cholesterol and DSTAP in molar ratio of 55:30:15 were weighted into a vial and dissolved with 2 ml of chloroform on a rotary evaporator under nitrogen gas. The vial was put in the vacuum oven for overnight for thin-film preparation. For hydration process, 1 ml of ammonium sulfate [$(NH_4)_2SO_4$] (250 mM, pH: 5.4) was added to the thin-film and put in the water bath for 1 hour at 65 °C at 150 rpm (Figure 3.3). The extrusion of the solution was done to produce liposomes. DOX loading process was done as active loading because of the ionic gradient inside and outside of the liposomes. First, liposomes were dialyzed against 1 L of 0.9% sodium chloride (NaCl) solution to replace $NH_4)_2SO_4$ on the exterior solution of the liposomes using dialysis membrane (Spectrum Laboratories, 10 kD MWCO). NaCl solution creates an osmotic pressure during the removal of the excess amount of ammonium sulfate. The setup was put on a magnetic stirrer and left overnight at room temperature (25 °C). Next day, 1 ml of liposome solution was taken from the dialyses bag, to which DOX solution at 1 mg/ml in UPW was added. The resulting solution was incubated in the water bath for 3 hours at 65 °C at 150 rpm. After loading process, unloaded DOX was separated from loaded liposomes (lipoDOX) by dialysis method as described above. Purified lipoDOX was stored at 4 °C for further use.

Figure 3.3. DOX loaded liposome production process.

3.2.8. Size and Zeta Potential Measurements of Liposomes

Particle size and zeta potential of liposomes were determined by dynamic light scattering technique using Malvern Zetasizer Nano ZS (Figure 3.4). Particles of liposomes make a characteristic Brownian motion in the solution which causes fluctuations on the laser beam and size distribution of the particles was obtained by analyzing the data. Commonly non-invasive visible light is used in DLS.

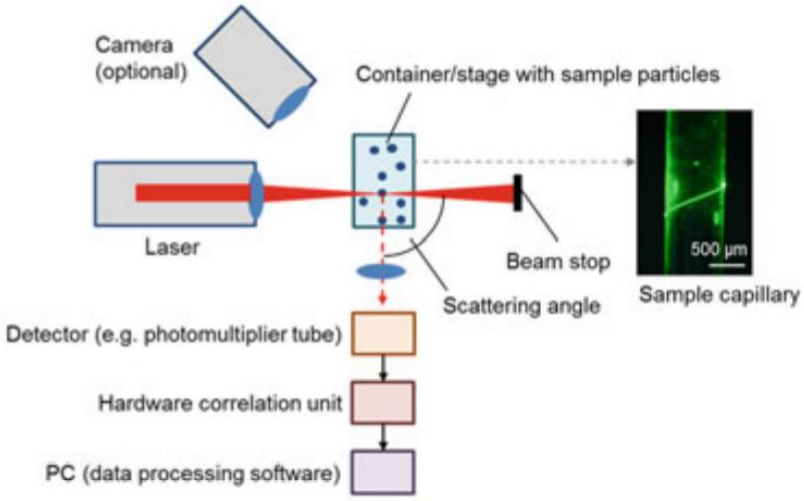

Figure 3.4. Dynamic Light Scattering (DLS) setup

Scattering light pattern auto corrects with their own data at correlation interval (τ) which is the data after a delay as shown in Figure 3.5. Decay time constants depend on the speed of the diffusion of particles. As the particle gets smaller, the decay time constant becomes shorter. Decay time constants come from exponential auto-correlation function (ACF) which is used for finding diffusion constant (D) by CONTIN algorithm. Temperature (T) is maintained constant during measurements and viscosity (η) of the solution is known. Stokes-Einstein equation (Eq. 3.3) gives the hydrodynamic radius (r_h) of the particle by substituting these known values in the formula. (k_B: Boltzmann constant 1.380648 × 10−23 J K^{-1})

$$D = \frac{k_B\, T}{6\pi\, \eta\, r_h} \qquad (3.3)$$

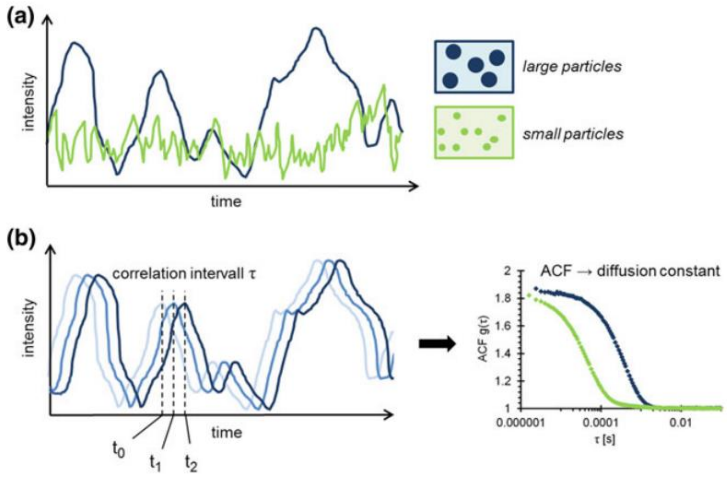

Figure 3.5. DLS mechanism (a) Brownian motion of the particles (b) Autocorrelation

The zeta potential of liposomes can provide not only the stability status of the liposomes but also it gives some important information about particle-particle interactions, particle-protein interactions, cell permeability of particles and biocompatibility. It depends on several conditions such as temperature, pH, conductivity which is ionic strength of the molecule and solvent viscosity.

Surface potential of a liposome describes as the highest potential and it is inversely proportional to distance as shown at Figure 3.6, which attracts the opposite charged ions. This opposite charged of ions called Stern layer and their potential called as Stern potential. The outer area after Stern layer called as Slipping plane, which contains the free ions, does not connect with the liposome. So, when liposome moves, free ions are not affected. Zeta potential describes the potential of the Slipping plane and the area between Stern layer and Slipping plane called electrical double layer.

In the Zetasizer, zeta potential measurements were done automatically by light scattering method. After the sample is put into the folded capillary zeta cell, which contains two gold electrodes, charged ions migrate to these electrodes by electrical stimulation. The migrating velocity of the ions is directly proportional to their zeta potential and by measuring the phase shift of the scattered light, zeta potential of the ions gets calculated with phase analysis light scattering (PALS). The calculations done by Henry Equation (Eq. 3.4) (Smith et al., 2017).

$$Ue = 2\,\varepsilon\, z\, f(\kappa a) / 3\eta \qquad (3.4)$$

where, U_e = Electrophoretic mobility

ε = Dielectric constant

z = Zeta potential

f (κa) = Henry function

κ = Debeye length (electrical double layer thickness)

a = radius of the particle

η = Absolute zero-shear viscosity of the medium

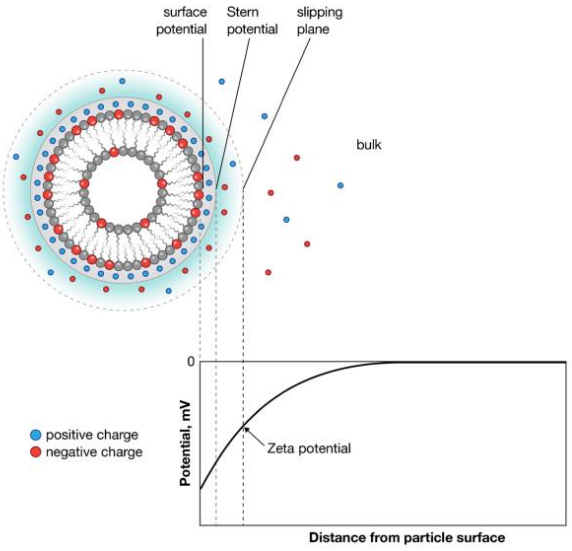

Figure 3.6. Zeta potential illustration of a negatively charged liposome.

Size and zeta potential values of loaded and unloaded liposomes were measured by Zetasizer (Malvern Nano-ZS) at 25 °C. For determining the most stable liposome concentration, different liposomes with different molar percent of DSTAP were prepared (0-5-10-15-20-25%) and their size and zeta potentials were measured in the medium of UPW/PBS (400 μL UPW + 580 μL PBS + 20 μL liposome solution). Flat bottomed cuvettes were used for size measurements and folded capillary zeta cell were used for zeta potential measurements.

Size and zeta potential changes of unloaded liposomes were monitored at 4 °C, 37°C and 25 °C by Zetasizer (Malvern Nano-ZS). For body (37 °C) and room temperature (25 °C) experiments, liposomes (undiluted) were put in water bath at desired temperatures. 20 μL samples were taken every 15 minutes in the first 1 hour and then every hour. For 4 °C experiments, liposome was kept at the refrigerator and the same process carried on. Later, liposomes for all temperatures were kept waited for 3 more hours and samples were taken at every hour.

3.2.9. Stability Control of Loaded Liposomes at Body Temperature

Size and zeta potential changes of loaded liposomes were also observed at body temperature (37 °C) by Zetasizer (Malvern Nano-ZS). 0.25 mg cholecalciferol ($VitD_3$) (10000 IU) containing liposome was used for the experiments and put into water bath at 37 °C and 150 rpm. Samples were taken every 15 minutes for 1 hour and every hour after that. During ongoing experiments, liposome was kept waited for 3 more hours, and samples were taken at every hour.

3.2.10. Determination of the Optimum Centrifugation Time for Liposomes

Unloaded $VitD_3$ was separated from the loaded liposomes by centrifugation as suggested by the literature (Dalmoro et al., 2019). For determining the optimum centrifuge time for the liposomes, 0.25 mg cholecalciferol ($VitD_3$) (10000 IU) containing 1 ml of liposome solution was aliquoted into 8 Eppendorf tubes as 100 µl. Tubes were subjected to centrifugation (Hettich Zentrifugen Mikro 220R) at 17000 rpm at 4 °C. One of the tubes was removed from the centrifuge at the predetermined times. Every sample's supernatant part was withdrawn and transferred into an opaque vial and 10 µL of it was mixed with 600 µl ethanol. Also, to the pellet remained in the tube, 600 µl of ethanol was added. The pellet was allowed for dissolution for 30 minutes then put in the sonic bath (WiseClean) for 1 minute at 20% amplitude. UV absorbance of both the pellet and supernatant were measured by UV-Vis Spectrophotometer (Perkin Elmer Lambda 25) at 265 nm.

3.2.11. Evaluation of $VitD_3$ Distribution Upon Centrifugation

To determine the distribution behavior of $VitD_3$ between the pellet and supernatant, a separate experiment was designed with $VitD_3$ dissolved in ethanol. 1.27 mg $VitD_3$ was dissolved in 100 µL of ethanol, resulting in 12.75 mg/ml stock concentration. Then, 2 µl of stock solution was putted on 7 different Eppendorf tubes and then, 100 µl of PBS was added on each one of them respectively. Tubes were subjected to centrifugation (Hettich Zentrifugen Mikro 220R) at 17000 rpm in 4 °C. One of the tubes was removed from the centrifuge every 15 minutes in the first 1 hour and every 30 minutes after 1 hour. and taken for absorbance measurement by UV-Vis Spectrometer

(Perkin Elmer Lambda 25) in every 15 minutes for 1 hour and every 30 minutes after 1 hour till complete 2 hours. According to the literature, $VitD_3$ would stay suspended in the PBS and unencapsulated $VitD_3$ could be removed with the supernatant for encapsulation efficiency measurements.

After centrifugation, 90 µl of supernatant of each sample was withdrawn as mimicking the liposome solution and 10 µL of it was dissolved in 600 µl ethanol. Also, 600 µl ethanol was added on the remained solution in the tube as mimicking the pellet. Their absorbance was measured, and concentrations were calculated from the calibration curve. Concentrations of the precipitate, supernatant, and initial concentration of tubes (before centrifugation) were evaluated after the experiment.

3.2.12. Effect of Cholesterol and $VitD_3$ on Liposome Production

Cholecalciferol and $VitD_3$ are similar in structure, and both are located in the bilayer of liposomes. In order to investigate the effect of cholesterol on $vitD_3$ loading, two different formulation series were designed. In one of the series, DSPC/cholesterol/DSTAP molar ratio was kept constant as 65:30:5 (total mole of the lipids DSPC and DSTAP is 15 µmol), but varying amounts of $VitD_3$ (Table 3.1) was added to the formulation in the series.

Table 3.1. Amounts of $VitD_3$ used in liposomes composed of DSPC, cholesterol and DSTAP at molar ratio of 65:30:5 (total mole of lipids is 15 µmol)

$VitD_3$, mole %	**n, µmole**
0.5	0.075
1	0.15
5	0.75
10	1.5
30	4.5
60	9

In the other series, varying amounts of cholesterol were added to the formulation which composed of DSPC, DSTAP at molar ratio of 65:5 (total mole of the lipids is 15 µmol) and constant amount of $VitD_3$ (0.28 mg) as shown in Table 3.2. Liposomes were prepared as explained before.

Table 3.2. Amounts of cholesterol used in the liposomes composed of DSPC, DSTAP at molar ratio of 65:5 (total mole of lipids is 15 μmol) and containing constant amount of $VitD_3$ (0.28 mg)

Cholesterol, mole %	**n, μmole**
30	4.5
20	3
10	1.5
5	0.75

10 μl of each liposome was dissolved in 600 μl ethanol and their absorbance were measured with UV-Vis Spectrometer (Perkin Elmer Lambda 25) to find the actual (UV measured) concentration of $VitD_3$ in liposomes. Then, 100 μl of each sample were put in an Eppendorf tube and centrifuged at 17000 rpm at 4 °C for 1 hour (Hettich Zentrifugen Mikro 220R). 90 μl supernatant was removed and transferred to another tube. 10 μl of the supernatant was dissolved in 600 μl ethanol and its absorbance was measured. 600 μl ethanol was added on 10 μl pellets remained in the tube. After vortex, its absorbance at 265 nm got measured as well. Concentrations of each sample were calculated by using the calibration curve. Sum of the $VitD_3$ mass in the supernatant and pellet of the same sample was obtained to check the mass balance. Theoretically, the sum of the $VitD_3$ mass in the pellet and supernatant are expected to be the same as the mass of $VitD_3$ in the liposomes prior to centrifugation.

Size and zeta potential measurements of each liposome were done by using Zetasizer (Malvern Nano-ZS) to control the stability of liposomes as explained before.

3.2.13. Encapsulation Efficiency

Encapsulation efficiency was determined by centrifugation method (Dalmoro et al., 2019). $VitD_3$ loaded liposomes, composed of 55% DSPC, 30% cholesterol and 15% DSTAP by molar mass, were prepared by thin-film method. The amounts of $VitD_3$ used were 0-0.07-0.12-0.23-0.51 mg, corresponding to approximately 0-2500-5000-10000-20000 IU (1 IU = 0.025 μg). First, prior to centrifugation, the amount of $VitD_3$ in liposomal formulation was determined. 10 μl of each liposome solution was dissolved in 600 μl ethanol and their absorbance was measured by UV-Vis Spectrometer (Perkin Elmer Lambda 25). UV measured $VitD_3$ weight was calculated by calibration curve

equation. Then, 100 µl of $VitD_3$ loaded liposome solution was taken into an Eppendorf tube and centrifuged (Hettich Zentrifugen Mikro 220R) for 60 minutes at 17000 rpm and 4 °C. The supernatant part (90 µL) was removed with pipet and transferred to an opaque vial. 600 µl ethanol was added onto the remaining 10 µl pellet in the tube and the solution was vortexed till the pellet got dissolved. After dissolving in ethanol, the pellet was kept waited for 30 minutes then, put in the sonic bath (WiseClean) for 1 minute at 20% amplitude. Absorbance of the sample was measured by UV-Vis Spectrometer (Perkin Elmer Lambda 25) and encapsulation efficiency was calculated as Eq. 3.5.

$$EE\% = (W_{Pellet} / W_i) \times 100 \quad (3.5)$$

where W_{Pellet} represents the total $VitD_3$ amount in the pellet after centrifugation and W_i represents the initial mass of $VitD_3$ added to the liposomes.

3.2.14. Fucoidan Coating on Liposomes

Four different liposomes with constant DSPC and cholesterol but different DSTAP percentage (0-5-10-20%) were prepared by thin-film hydration method. Liposomes of 450 µl of each was transferred to 2 ml vials. 9 mg fucoidan (FUC) from *Fucus vesiculosus* was weighted and dissolved in 5 ml PBS to prepare FUC stock solution (1.8 mg/ml). To each liposome in the vials, 10 µl of FUC solution was added. After sample was mixed with a vortex mixer (WiseMix), another 10 µl of FUC stock solution was added into the sample and the sample was mixed again. By this way, total 20 µl of FUC stock solution was added into the sample. After mixing process, size and zeta potential measurements of sample was done by Zetasizer (Malvern Nano-ZS). FUC stock solution and FUC stock solution added liposomes were kept on mixer during the experiments. Additional 20 µl FUC stock solution was added on liposomes in similar manner and the zeta potential of the liposomes was measured again. FUC stock solution addition process was repeated till the zeta potential of liposomes dropped to negative values and stayed constant. Same process was done with 450 µl PBS solution to observe the FUC behavior in water.

3.2.15. Fucoidan Coating of Loaded Liposome

Five different liposomes composed of DSPC, cholesterol and DSTAP at molar % (55:30:15) but with different amount of cholecalciferol ($VitD_3$) (0-0.07-0.12-0.23-0.51 mg, corresponding to approximately 0, 2500 IU, 5000 IU, 10 000 IU and 20 000 IU))

were prepared as explained above. From each Liposome, two Eppendorf tubes containing 200 µL of each liposome were prepared as bare liposomes and FUC coated liposomes (Figure 3.7) (2 x 5 = 10 Eppendorf tubes).

For fucoidan (FUC) coating, 0.35 mg FUC from *Fucus vesiculosus* was weighted and dissolved in 1 ml distilled water as stock solution. Then, FUC stock solution was diluted by 1/2, 1/4, 1/8, 1/16 ratio with distilled water. 10 µl of FUC stock solution was added into each vial containing 200 µL of the liposomes with different amounts of $VitD_3$. Another 200 µl of 0.51 mg $VitD_3$ (20000 IU) containing liposome was taken into an Eppendorf tube and diluted with PBS as the same ratio of FUC stock solution. 10 µl of FUC solutions with same dilution ratios were added on the liposomes with same dilution ratio.

Doxorubicin (DOX) loaded liposomes composed of DSPC, cholesterol and DSTAP at molar ratio of (55:30:15) were prepared and separated into 2 Eppendorf tubes as 200 µl. 10 µl of FUC stock solution was added on each of them (Figure 3.7).

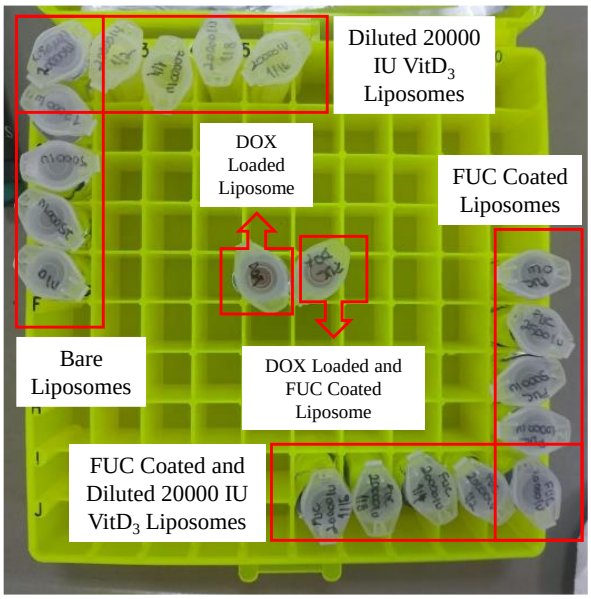

Figure 3.7. $VitD_3$ and DOX loaded bare and FUC coated liposome preparation setting.

3.2.16. $VitD_3$ Pretreatment on MDA-MB-231 Cells

100 mg cholecalciferol ($VitD_3$) was dissolved in 2 ml of ethanol and filtered. MDA-MB-231 breast cancer cells were produced in 25 cm^2 flasks and after reaching 90% confluency (Figure 3.8), they were scrubbed by a cell scrubber from the flasks. Then, cells were put into centrifugation for 7 minutes at 200 rpm. The pellet was taken to another

tube and suspended by 1 ml DMEM (Dulbecco's Modified Eagle Medium). Trypan blue was added into the solution at 1:1 ratio in an Eppendorf tube then put on Thoma Lam (ISOLAB), and cells were counted under the microscope (OLYMPUS CKX41). Average viable cell count per square for cell cultivation was calculated by Eq. 3.6.

Total cell number x Dilution factor x 10^4 = Average viable cell count per square (3.6)

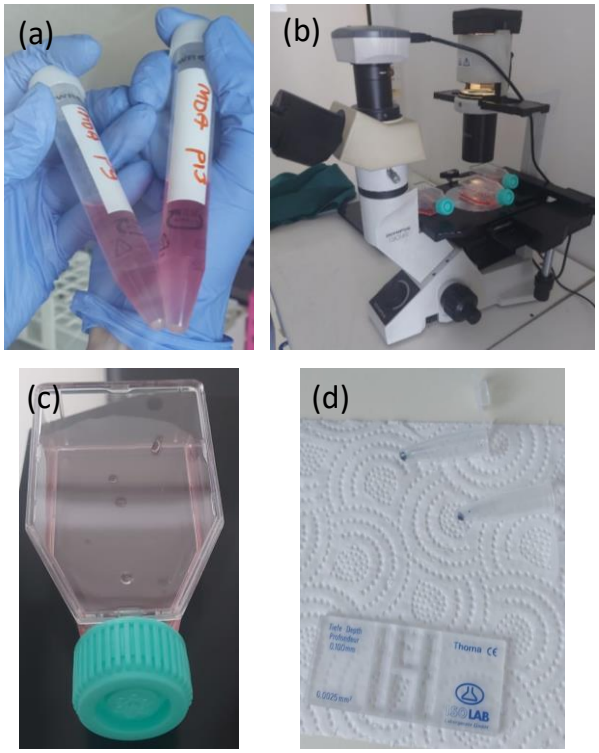

Figure 3.8. a) Pellet after centrifugation, b) Cell control, c) Cell culture in flask, d) Thoma Lam for cell counting.

Cells were cultivated on 3 different 96-well plates for 24-, 48- and 72-hours observation and kept waited in the incubator at 36 °C. Next day, 0-5-50-100 µM $VitD_3$ was treated on the cells in both 3 different well plates and put back to the incubator (Fig. 3.13) (Kutlehria et al., 2018). After 24 hours, 20 µl of MTT (3-(4,5-dimethylthiazol-2-yl)-2,5-diphenyl tetrazolium bromide) dissolved in PBS and sterilized was added on the cells in 1 plate and put in the incubator for 4 hours (Fig. 3.14). At the end of 4^{th} hour, the mediums in the cells were withdrawn and added 50 µl dimethyl sulfoxide (DMSO) and kept waited in the incubator. Then, well plates were analyzed in ELISA (Biotek, Synergy HT) at 590 and 630 nm, since MTT has an absorption at these wavelengths (Fig. 3.15). The same process was applied for all the well plates for 48 and 72 hours.

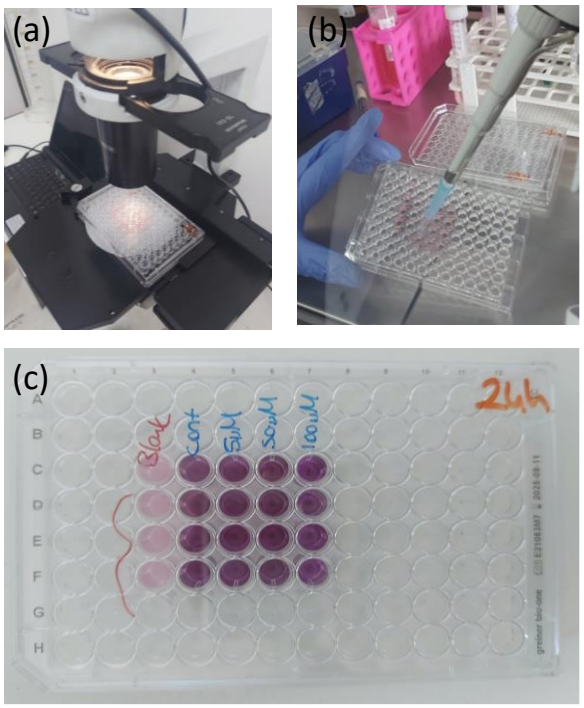

Figure 3.9. a) $VitD_3$ added cells on 96-Well plate for 24 hours of observation, b) MTT assay, c) DMSO added well-plate for ELISA.

3.2.17. DOX and $VitD_3$ Treatment on MDA-MB-231 Cells

Human breast cancer cell MDA-MB-231 was reproduced by adding 10% fetal bovine serum (FBS), 2 mM L-glutamin and 100 international unit (IU) pensilin/streptomisin into their DMEM media at 37 °C and 5% CO_2 incubator environment for twice a day. MTT (3-[4,5-dimetiltiyazol-2-il]-2,5-difenil-tetrazolyum bromide) was used for cell viability test. For determine the cholecalciferol ($VitD_3$) and doxorubicin (DOX) concentrations for the cell treatment, different amounts of doses were treated on the cells that planted on the 96-well plates for 24-, 48- and 72-hours. $1x10^5$ cells were planted on every single well and waited for 24 hours to get reproduced. After 24 hours, $VitD_3$ (0-3.125-6.25-12.5-25-50-100 µM) and DOX (0.1-1 µM) concentrations were treated on the cells. For combination groups (DOX + $VitD_3$) first $VitD_3$ was treated on the cells and after 30 minutes DOX was treated on the same cell.

After cells were treated with DOX and $VitD_3$, 20 µl MTT was added on every well and incubated at 37 °C for 4 hours. At the end of the fourth hour, 50 µl DMSO was added on the wells and after 15-30 minutes their absorbances were measured at 590-630 nm at ELISA (Biotek, Synergy HT). Viability of cells were evaluated according to the control groups by %. Every condition was repeated at least 3 times.

3.2.18. Fucoidan Coated and Uncoated $VitD_3$ Loaded Liposome Treatment on MDA-MB-231 Cells

For this part of the study, fucoidan (FUC) coated and uncoated $VitD_3$ and DOX loaded liposomes were treated on the MDA-MB-231 cancer cells. Also, for DOX loaded liposome treatment, cells were pretreated with $VitD_3$ before liposome treatment.

Cancer cells were grown in 10% FBS, 1% pen-strep and l-glutamine contained DMEM (Dulbecco's Modified Eagle Medium) solution at 37 °C with 5% CO_2. When cells reached 90% confluency, they were scraped and put on the centrifuge for 7 minutes at 4 °C and 1500 rpm. After pellet formation, supernatant was removed, and pellet was dissolved in 1 ml DMEM. Then, cell counting assay was performed with tryphan blue (1:1) and cells were planted on 96-well-plates. There were 10000 cells in each well and 3 plates were used for 24-48-72 hours of observation. After 24 hours, plates were controlled under microscope (OLYMPUS CKX41) and fucoidan coated and uncoated liposomes (0-0.07-0.12-0.23-0.51 mg/ml $VitD_3$ + 0.35 mg/ml FUC, 0.26 mg/ml $VitD_3$ + 0.18 mg/ml FUC, 0.13 mg/ml $VitD_3$ + 0.09 mg/ml FUC, 0.06 mg/ml $VitD_3$ + 0.04 mg/ml FUC, 0.03 mg/ml $VitD_3$ + 0.02 mg/ml FUC, 1 mg/ml DOX + 0.35 mg/ml FUC, 1 mg/ml DOX) were treated on cells with 90% confluency. For DOX loaded liposome treatment, cells were pretreated with 100 µM $VitD_3$ (dissolved in ethanol) for 30 minutes.

After 25 hours of liposome treatment, images of cells were taken and 20 µl 3-(4,5-dimethylthiazol-2-yl)-2,5-diphenyl tetrazolium bromide (MTT) was added on the wells for 4 hours. Then, medium inside the plate was withdrawn and 50 µl DMSO was added on the cells. After 30 minutes, plates were analyzed in ELISA (Biotek, Synergy HT).

CHAPTER 4

RESULTS AND DISCUSSIONS

4.1. Liposome Production and $VitD_3$ Loading

Liposomes were produced by thin-film method and stored at refrigerator at 4 °C for maximum 1 week because of the short storage life of cholecalciferol ($VitD_3$) (Figure 4.1). The ones loaded with $VitD_3$ were protected against light using opaque vials and aluminum foil. In liposome making, DSPC was used for creating spherical liposomal structures. Cholesterol was used to increase stability and diffusion across its membrane. DSTAP was used as cationic lipid to create a positive charge on the surface of liposomes. $VitD_3$ was loaded into liposomes passively since it's a liposoluble/hydrophobic molecule and has a poor water solubility.

Figure 4.1. $VitD_3$ loaded liposome.

4.2. Size and Zeta Potential Measurements of Unloaded Liposomes

Before the loading process of cholecalciferol ($VitD_3$) into the liposomes, stability of empty liposomes composed of at different mol% of DSTAP were investigated by measuring their size and zeta potential.

Liposomes composed of 0-5-10-15-20-25 mole% DSTAP while keeping the cholesterol content constant at 30% were prepared and their size and zeta potential were measured in the medium composed of 400 µl PBS + 590 µl UPW at 25 °C. As seen in the Figure 4.2, zeta potential of the liposomes increased with DSTAP percentage up to

20%, further increase in DSTAP % did not result a significant change in zeta potential. In Dabbas et al. studies, zeta potential of liposomes with 10% lipid content of DSTAP measured as 8.9 ± 4.2 mV and 25% DSTAP measured as 17.4 ± 1.9 mV in distilled water (Dabbas et al., 2008). Even though liposomes were prepared with different DSTAP percentages, there was no significant change in the size of liposomes. Liposomes exhibited a size around 200 nm, which is very similar to the size of polycarbonate membrane used during the extrusion process. This result showed that pore size of the polycarbonate membrane determined the size of the liposomes and liposome composition or DSTAP percentage had no effect. Liposomes with size of around 200 nm is considered an optimum size for liposome to get through the leaky endothelial of the tumor cells.

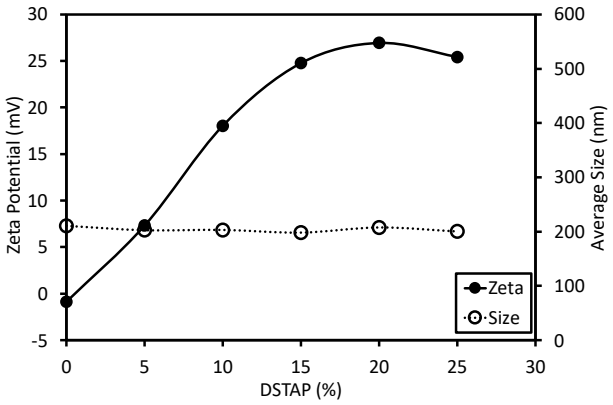

Figure 4.2. Average size and zeta potential of unloaded and different DSTAP mole percentage involved liposomes in 400 µl PBS + 590 µl ultrapure water.

4.3. Size and Zeta Potential Measurements of Loaded Liposomes

The higher the zeta potential of the liposomes, the higher amount of fucoidan can be coated onto liposomes, which is need for binding of liposomes to p-selectins expressed in cancerous tissues. According to these results, liposomes with 15-20% DSTAP could be good choice when considering the fucoidan coating. Therefore, in the subsequent study, varying amounts of $VitD_3$ was loaded into liposomes composed of DSPC/Cholesterol/DSTAP at molar ratio of 55:30:15 and effect of loading on the size and zeta potential of liposomes was investigated. As seen from Figure 4.3, the size of the loaded liposomes remained constant at around 200 nm, indicating that the pore size of the polycarbonate membrane is very decisive in the size of resulting liposome after extrusion. The zeta potential of loaded liposomes also did not change with loaded amount of $VitD_3$, exhibiting almost the same zeta potential with the unloaded liposomes (around 25 mV).

From the size and zeta potential measurements, it may be concluded that encapsulation of $VitD_3$ into the bilayer of liposomes (since $VitD_3$ is a lipophilic molecule) did not cause an alteration in the structure of liposomes for $VitD_3$ in the concentration range studied.

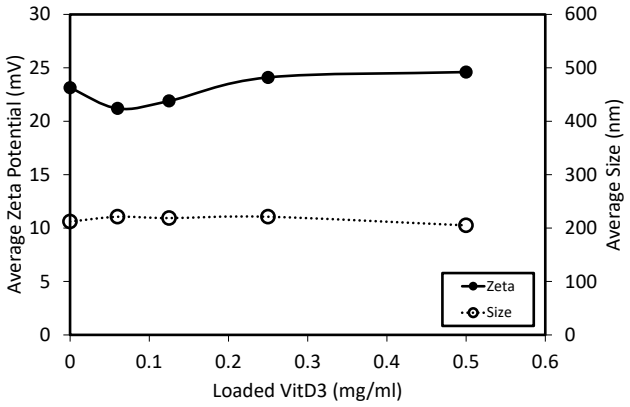

Figure 4.3. Average size and zeta potential measurement of $VitD_3$ loaded liposomes with 15 moles % DSTAP in 400 µl PBS + 590 µl ultrapure water (UPW)

4.4. Temperature Stability of Liposomes

It is necessary to observe liposomes stability changes at different temperatures to observe their behaviors under different circumstances. For stability control experiments, liposomes were incubated at 4 °C, 25 °C and 37 °C, which are corresponding to possible storage temperature, room temperature, and body temperature, respectively. At 4 °C, zeta potential and size measurement of the liposomes were done before they were put in the refrigerator and after 3-month storage at the refrigerator. Figure 4.4.(a) shows the change in the size of liposomes with different DSTAP mole% after 3 months. As seen, there was a slight increase in size of the liposomes after three months and this increase is much more pronounced with liposomes with higher DSTAP contents. Despite this, zeta potential of the liposomes remained almost unchanged (Figure 4.4.(b)). At room and body temperatures, samples were withdrawn from the vial every 15 minutes in the first one hour and every hour afterwards. The size and zeta potential of the liposomes with different DSTAP mole% did not show a significant change over time interval studied at both temperatures (Figure 4.4.(c)-(f)). The sizes were decreasing, and the zeta potential values were decreasing at increasing temperatures for each liposome studied.

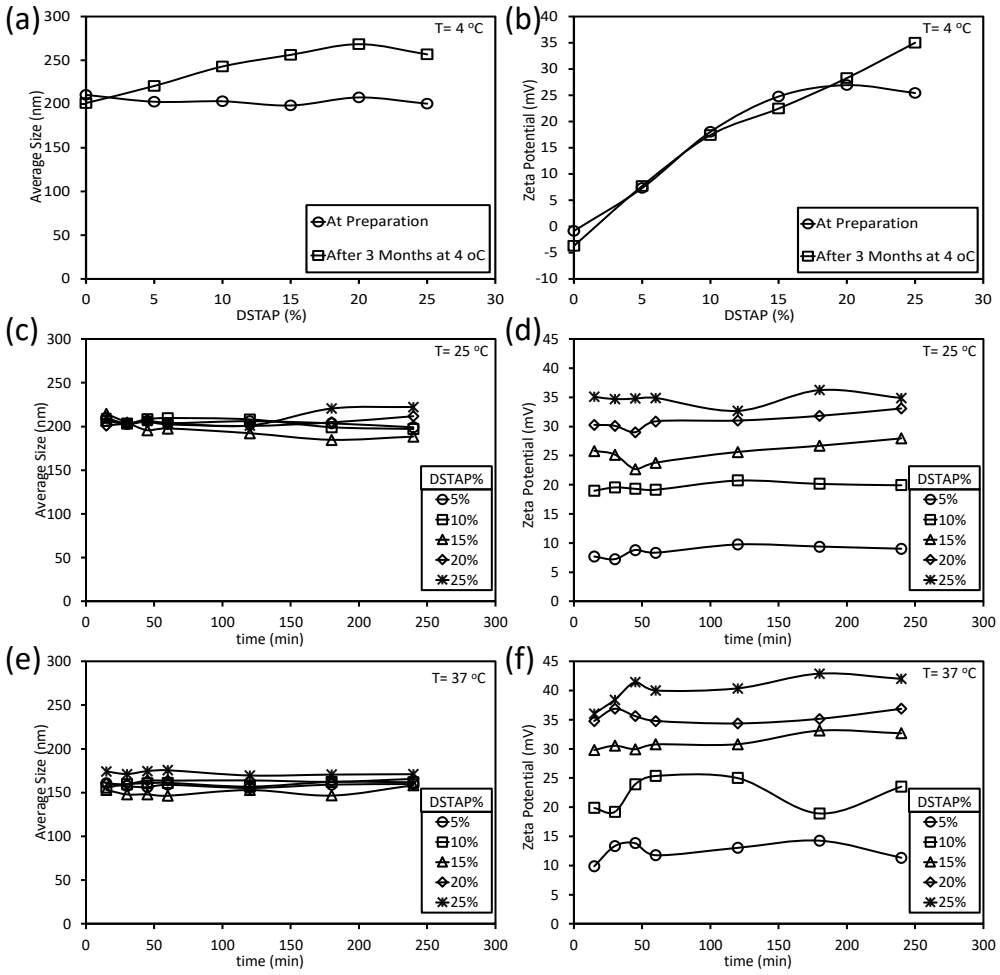

Figure 4.4. Average size and zeta potential measurements of unloaded liposomes at different temperatures (a-b) 4 °C (c-d) 25 °C (e-f) 37 °C (Note: all size and zeta potential measurements were done in 400 µl PBS + 590 µl ultrapure water)

The temperature effect on the size and zeta potential of liposomes can be clearly seen in Figure 4.5. For the 20 moles% of DSTAP liposomes, size of the liposomes decreased while their zeta potential increased with increasing temperature. Other liposomes having different mole% DSTAP contents also exhibited similar behavior. Having observed liposome shrinkage at 37 °C in fetal bovine serum, Wolfram et al. suggested that osmotic pressure can cause the shrinkage and this may lead to the drug release (Wolfram et al., 2014).

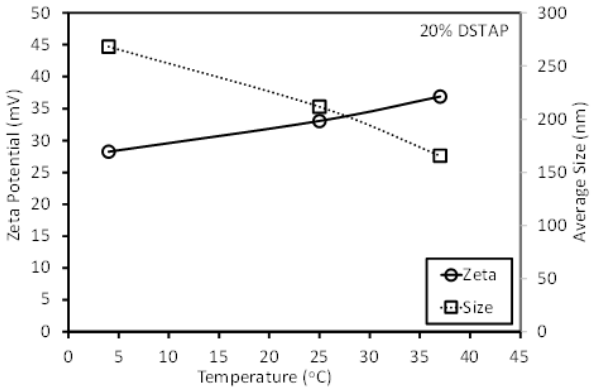

Figure 4.5. Effect of temperature on size and zeta potential of liposomes containing 20 moles% of DSTAP as an example

These results indicated that liposomes are more stable at 4 °C and thus they can be stored at this temperature until further use. Combination of the results depicted in Fig. 4.3 and Fig 4.4 (a)-(b) may suggest that $VitD_3$ loaded liposomes can be stored at 4 °C for some time. Indeed, Chen et.al exposed $VitD_3$ coated Fluoropak 80 powders to air and water. They observed a change in their absorbance. They concluded that $VitD_3$ can be stored in the refrigerator because of its stable absorbance data at 4 °C (Chen et al., 1965).

Temperature stability of the loaded liposomes was investigated at 37 °C. Liposomes with 15mole% DSTAP were loaded with $VitD_3$ (0.25 mg, equivalent to 10.000 IU) was incubated at 37 °C, and their size and zeta potential values were measured. Figure 4.6 shows the average size and zeta potential of $vitD_3$ loaded liposomes. Neither size nor the zeta potential of the liposomes had changed during the incubation at 37 °C, suggesting that $VitD_3$ loaded liposomes can be used in the *in vitro* and *in vivo* studies.

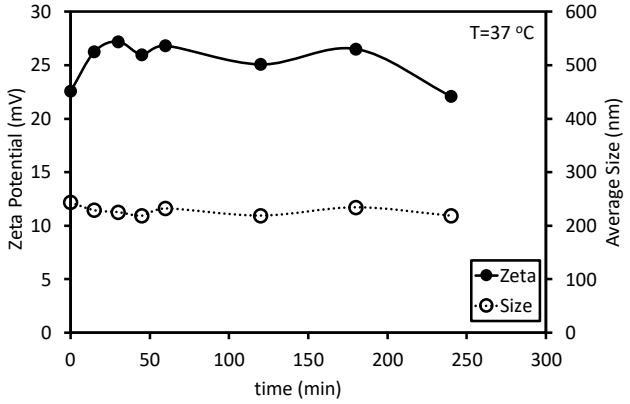

Figure 4.6. Average size and zeta potential measurements of 0.25 mg $VitD_3$ loaded (10000 IU) liposome at 37 °C (1 IU = 0.025 µg)

4.5. Quantification of $VitD_3$ Using UV-Vis Spectrophotometry

UV-vis spectrophotometry was used to determine the amount of cholecalciferol loaded into liposomes. According to the supplier, it is known that cholecalciferol has a high solubility in ethanol (around 50 mg/mL, Sigma-Aldrich Inc.). Therefore, in order to determine the wavelength at which the cholecalciferol exhibits the maximum absorbance, the absorbance scan was obtained for the cholecalciferol and other components. As seen in Figure 4.7, cholecalciferol absorbs UV light at around 265 nm as the maximum, which is in agreement with the literature (Japelt and Jakobsen, 2013). In order to make sure if there is any interference from the other components in the solution, absorbance-wavelength spectra of phosphate buffer saline (PBS), ultra-pure water, solution of liposomes in ethanol and liposome in water were also measured. As seen from the figure, liposomes in water have absorbance due probably to light scattering. Liposomes were seen to dissolve in EtOH and show absorbance slightly due to scattering from lipids. PBS has slight absorbance due to phosphate ions in the solution. Water has negative absorbance with respect to EtOH as the blind solution.

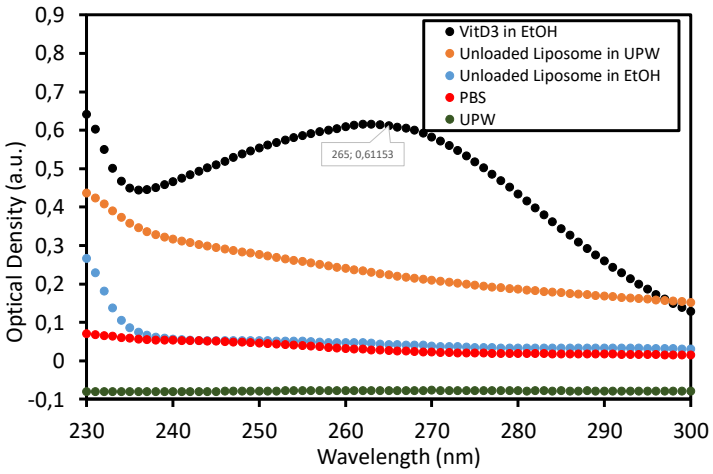

Figure 4.7. UV spectrum of $VitD_3$ and other components with liposomes.

4.6. Temperature Stability of $VitD_3$

In hydration process during liposome preparation, water bath temperature was set to 65 °C, a temperature 10 °C higher than the transition temperature of the main lipid, DSPC. Since $VitD_3$ was loaded into liposomes by passive loading at this hydration temperature, its stability was of concern. In order to make sure its stability during hydration process, $VitD_3$ solution in ethanol (0.1 mg/ml stock solution) was incubated in

water bath at 65 °C and its absorbance was measured at different times. As seen from Figure 4.8, absorbance values of the $VitD_3$ at different time intervals remained almost the same, indicating the stability of $VitD_3$ during hydration process.

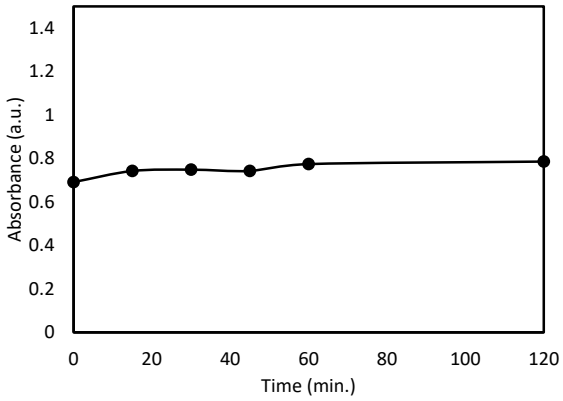

Figure 4.8. Temperature Stability of $VitD_3$ at 65 °C

4.7. Effect of Lipid Concentration on $VitD_3$ Absorbance

Cholecalciferol ($VitD_3$) was passively loaded into the liposomes and the effect of lipid concentration on absorbance measurement was of concern for further analysis. In order to make sure if the lipid mixture could affect the $VitD_3$ absorbance, mixture of DSPC + cholesterol + DSTAP was prepared at the same composition with the liposome studied and dissolved in ethanol. The final mixture was diluted to predetermined concentrations, and then the same amount of $VitD_3$ dissolved in ethanol was added into these lipid mixtures. As shown in Figure 4.9, there was not a significant change in the absorbance value of $VitD_3$ in the presence of liposome components.

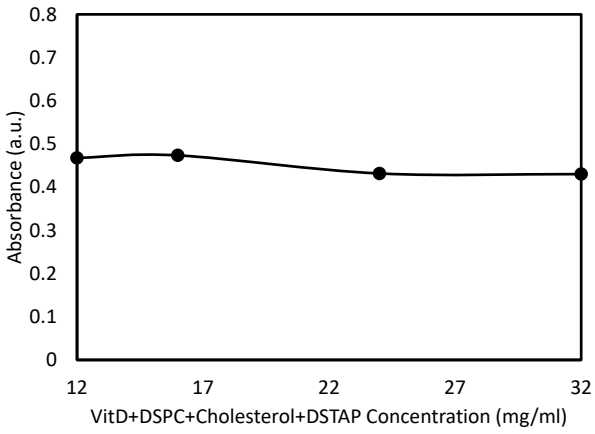

Figure 4.9. Effect of liposome mixture concentration on $VitD_3$ absorbance in ethanol.

4.8. Effect of PBS Solution on UV Absorbance of $VitD_3$ in EtOH

During quantification of loaded amount of $VitD_3$ in the liposomes by UV method, presence of PBS in the measurement medium is unavoidable because liposomes were prepared in the PBS solution. To understand if the presence of PBS in ethanol interferes with the absorbance of $VitD_3$, full spectra of PBS-EtOH mixtures at different volume ratios were investigated. Addition of different amounts of $VitD_3$ dissolved in ethanol into these PBS-EtOH mixtures were also investigated. Table 4.1 shows the mole fraction of ethanol, y_{EtOH}, and the corresponding volumes of PBS and ethanol in the mixtures. Pure ethanol was used always in the reference cell during UV measurements.

Table 4.1. EtOH mole fraction and the corresponding volumes of PBS and Ethanol (on 10 ml basis)

EtOH Mole Fraction (y_{EtOH})	**PBS:EtOH Volume Ratio (ml/ml)**
1.00	0:10
0.90	0.33:9.67
0.81	0.72:9.28
0.71	1.18:8.82
0.61	1.72:8.28
0.52	2.37:7.63
0.42	3.18:6.82
0.32	4.21:5.79
0.22	5.55:4.45
0.12	7.37:2.63
0.02	10:0

Full spectrum of PBS-Ethanol mixtures in the wavelength range of 200-360 nm was shown in Figure 4.10.(a). As seen from the figure, absorbance of the mixtures changed disorderly with ethanol mole fraction. Full spectrum of $VitD_3$ added at constant amount (dissolving in ethanol) into these PBS-Ethanol mixtures are shown in Figure 4.10.(b). Spectra of $VitD_3$ added at constant amount to these PBS-Ethanol mixtures also showed different behavior although the added amount of $VitD_3$ was constant in all PBS-Ethanol mixtures (Fig. 4.10.(b)), exhibiting the effect of background on $VitD_3$ absorbance. Spectra of $VitD_3$ can be extracted by subtracting the corresponding background from the spectra of mixtures containing $VitD_3$, as shown in Figure 4.10.(c). As seen in Figure 4.10.(d), measured absorbance value of $VitD_3$ at 265 nm would be

affected by the background absorbance, varying with the ethanol mole fraction. Figure 4.10.(e) shows the $VitD_3$ spectra in EtOH-PBS mixtures at 265 nm, their corresponding background and the spectra for $VitD_3$. As can be seen from the figure that, the same amount of $VitD_3$ could be detected although ethanol mole fraction varied. Other concentrations of $VitD_3$ were also obtained by subtracting their corresponding background as shown in Figure 4.10.(f). The result suggests that correct amount of $VitD_3$ can be determined by subtraction of background absorbance if the ethanol mole fraction is known. Also, notice that the background is almost none when ethanol mole fractions are higher than 0.9, or ethanol volume percent is higher than 96%. Therefore, it would be a better practice if the amount of $VitD_3$ concentrations could be measured at these solutions indicated.

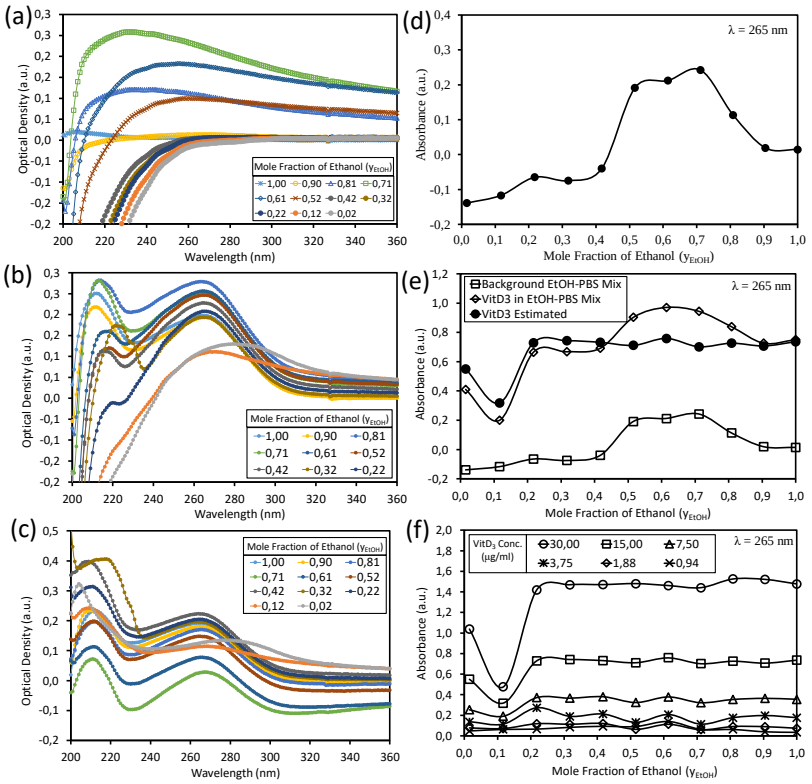

Figure 4.10. UV spectra of PBS-EtOH mixtures at different mole fractions of Ethanol, (a) not contained $VitD_3$ (b) contained same amount of $VitD_3$ (c) UV spectra of $VitD_3$ obtained by subtracting these two, and Absorbance of PBS-EtOH stock solutions at 265 nm (d) background (e) absorbance of $VitD_3$ after excluding the corresponding background (f) Absorbance of $VitD_3$ at different concentrations estimated by subtracting corresponding background absorbance at the wavelength of 265. Reference cells contain pure ethanol in all measurements.

Absorbance of different $VitD_3$ concentration in different PBS-Ethanol mixtures were measured and calibration curves for each was obtained as shown in Figure 4.11. Changes in the mole fraction of ethanol affected the calibration curves. Location of calibration curves shifted upwards till y_{EtOH} = 0.71 but after this point they shifted downwards but exhibiting a similar slope. Calibration curves produced using pure ethanol and PBS-Ethanol solution at y_{EtOH} = 0.90 almost overlapped, indicating presence of no interference from the background at y_{EtOH} = 0.90 during $VitD_3$ UV measurements. All these results suggest that $VitD_3$ in liposomes can be quantified by UV spectrophotometer as long as the ethanol content is higher than 90 moles% in the measurement medium.

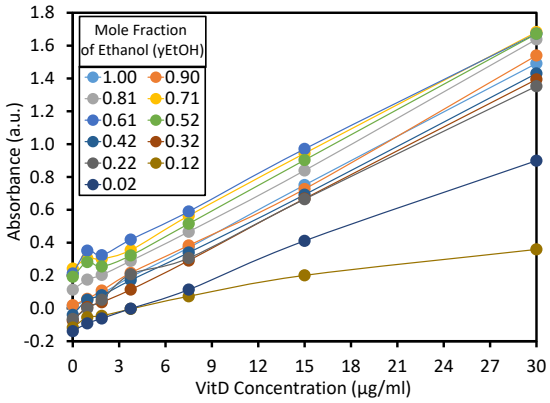

Figure 4.11. Calibration curves of $VitD_3$ in different PBS-Ethanol mixtures at 265 nm.

The calibration curves produced in pure ethanol and PBS-ethanol mixture at 90% ethanol mole fraction have very similar line equations as shown in Figure 4.12, indicating that either calibration curve can be used in quantification of $VitD_3$ loaded in the liposomes.

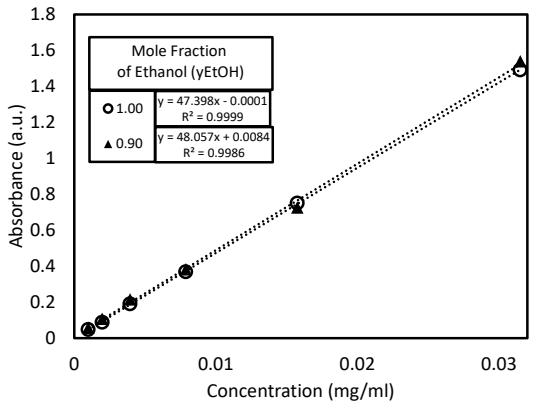

Figure 4.12. Calibration curves of $VitD_3$ in pure ethanol and in a mixture of PBS-Ethanol at 265 nm

4.8. Separation of Unloaded $VitD_3$ by Centrifugation

From the literature, it was seen that unloaded $VitD_3$ can be separated from the liposomes by centrifugation. Dalmoro et al. set the centrifugation time to 60 minutes at 35000 rpm using 3 ml sample (Dalmoro et al., 2019). However, the available centrifuge in our lab has an upper limit of 17500 RPM; and therefore, the time period needed to be optimized. In order to determine the distribution behavior of $VitD_3$ between the pellet and supernatant upon centrifugation, 100 μL of liposome samples were taken in Eppendorf tubes and inserted in the centrifuge. Gravitational force was applied at 17000 RPM at 4 °C. At each time interval, the centrifuge was suspended and one of the tubes was withdrawn. About 90 μL of supernatant was removed as supernatant. The remaining part, about 10 μL, was treated as pellet. Figure 4.13 shows the liposomes in the pellet and solution in the supernatant. It can be seen from the figure that the liposomes and supernatant can be separated from each other.

Figure 4.13. Pellet (at the bottom) and supernatant (at the top) after centrifugation.

The liposome sample was measured by the UV absorption at 265 nm and considered as the total $VitD_3$ content in liposome samples. The pellet and supernatant were measured in ethanol and $VitD_3$ contents were estimated in pellet and supernatant after correcting for the background UV intensity from ethanol-PBS mixture. Figure 4.14 shows the $VitD_3$ contents estimated in the pellet and the supernatant at different centrifugation time, and their total. It can be seen that while the $VitD_3$ content in the supernatant decreases, the $VitD_3$ content in the pellet increases and becomes stable after an hour or so. The estimated total amount of $VitD_3$ content is almost the same as the initially measured $VitD_3$ content in the sample. Thus, the $VitD_3$ estimation from the liposomes can be achieved by centrifuging the liposome samples for about 1 hour. This data is consistent with Dalmoro et al. as they set the centrifugation time to 60 minutes at 35000 rpm for 3 ml sample (Dalmoro et al., 2019).

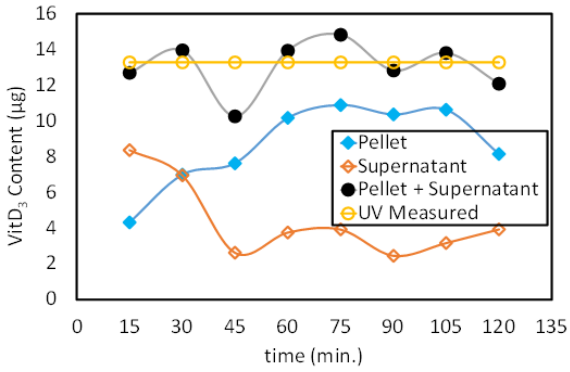

Figure 4.14. Pellet and supernatant absorbance measurements after centrifugation in ethanol.

In order to verify the distribution of $VitD_3$ between the pellet and the supernatant, liposomes with different amounts of $VitD_3$ were prepared. To the lipid mixture composed of DSPC/Cholesterol/DSTAP at molar ratio of 65:30:5, varying amounts of $VitD_3$ were added and the liposomes were produced as explained in the experimental section. Each sample was centrifuged at 17000 rpm at 4 °C for 60 minutes and then the pellet and supernatant phases were separated. Absorbance of the pellet and the supernatant in ethanol was measured, keeping the ethanol content higher than 90 moles% (or 96 volumes%) in the measurement medium. Absorbance measurements of the phases showed that the pellet containing $VitD_3$ loaded liposomes was richer in $VitD_3$ while small amount of $VitD_3$ was detected in the supernatant (Figure 4.15), in agreement with the study of Dalmoro et al. (Dalmoro et al., 2019). Summation of the $VitD_3$ contents in the pellet and the supernatant was found to be close to the $VitD_3$ detected in the liposome prior to centrifugation.

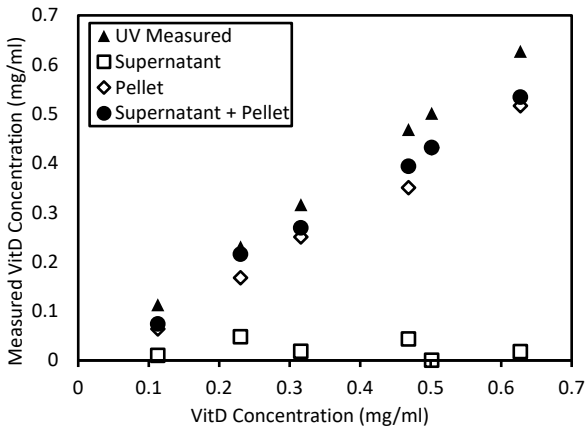

Figure 4.15. Distribution behavior of $VitD_3$ between the pellet and the supernatant upon centrifugation of the liposomes

4.9. Liposomes Loaded with Cholesterol and $VitD_3$

Cholesterol was used in liposome making process to get stable liposomes for drug release. Since cholesterol and $VitD_3$ are lipophilic molecules, they both locate in the bilayer of liposomes. Molecular structures and UV spectrum between 200 and 300 nm for cholesterol and $VitD_3$ are shown in Figure 4.16. As seen, cholesterol does not have a specific absorbance at 265 nm, which does not affect the estimation of $VitD_3$ by UV method. Also, both $VitD_3$ and cholesterol have identical side chains C and D in their formula and this side of the molecules also similar as enzyme binding capacity which is the reason for $VitD_3$ to called as a steroid hormone (Tyler et al., 1968).

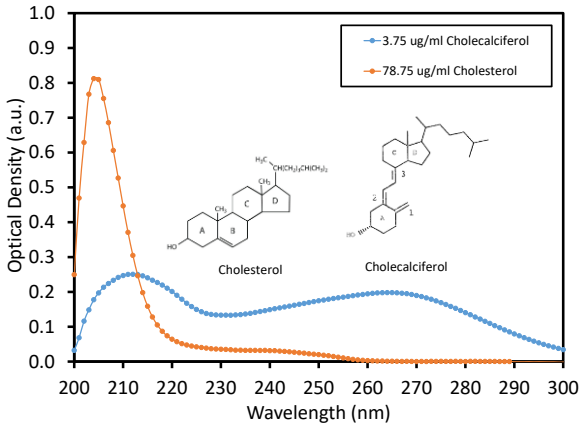

Figure 4.16. $VitD_3$ vs Cholesterol spectrum in ethanol and their molecular structure.

To test their effect on the liposome properties, two different formulation series were prepared. In one series, $VitD_3$ was added at different molar% to the liposomes with molar ratio of DSPC/Chol/DSTAP: 65/30/5. In the other series, cholesterol was added at different molar% to the liposomes composed of DSPC /DSTAP: 65/5, containing 5 moles% of $VitD_3$ (of the total lipids). It is important to note here that $VitD_3$ loaded liposomes could not be produced in the absence of cholesterol in the formulation. This result may suggest that $VitD_3$ locates in the interstices created by cholesterol in the bilayer. $VitD_3$ may also aggregate with the lipids and could not pass the membrane during extrusion process. As seen from Figure 4..(a), zeta potential of the liposomes increased from about 15 mV to 25 mV with increase of cholesterol content from 5 to 10 mole% and then remained almost unchanged with further increase in the cholesterol content. On the other hand, zeta potential of the $VitD_3$ liposomes decreased with increasing $VitD_3$ mole%. The sizes of the liposomes in either formulation series did not change significantly,

indicating that pore size of the polycarbonate membrane used during the extrusion process determined the size of the liposomes Figure 4..(b).

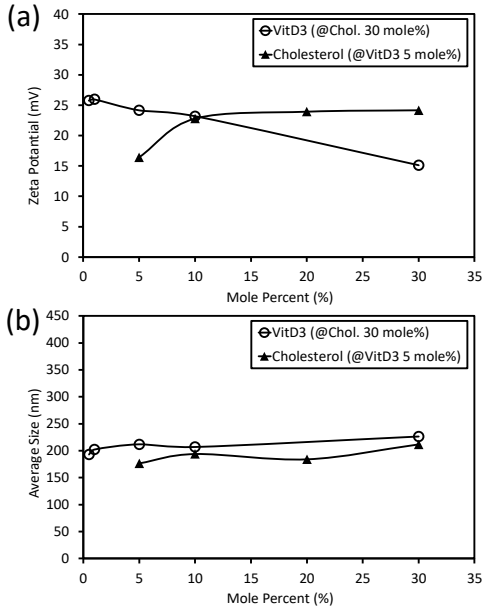

Figure 4.17. (a) Zeta potentials and (b) Size measurements of the liposomes composed of DSPC/Chol/DSTAP with varying cholesterol and $VitD_3$ contents.

4.10. Encapsulation Efficiency of Liposomes for $VitD_3$

Different amounts of $VitD_3$ were encapsulated within liposomes by the extrusion method. The loaded amount of $VitD_3$ was estimated with the UV absorbance at 265 nm in ethanol. The amount added during encapsulation and the amount estimated after liposomes were made resulted in encapsulation efficiency (EE%), and calculated using Eq. 3.5, where W_{Pellet} represents the total $VitD_3$ amount in the pellet after centrifugation and W_i represents the initial mass of $VitD_3$ added to the liposomes. Figure 4.17 shows the encapsulation efficiency of liposomes for $VitD_3$ which decreases with the increasing amount of $VitD_3$ loaded to the liposomes. The decrease in encapsulation efficiency is due probably to the retention of $VitD_3$ by the membrane during the extrusion process, causing some of $VitD_3$ to be lost during the extrusion process and thus loaded amount of $VitD_3$ to decrease. On the other hand, the liposome solution with 30% $VitD_3$ in the absence of cholesterol was unable to pass through the extrusion membrane, indicating that lipids were aggregated with $VitD_3$ and did not pass through the membrane in the extruder. As shown in the figure, about 70% encapsulation efficiencies were obtained with 0.5 mg of $VitD_3$ loading.

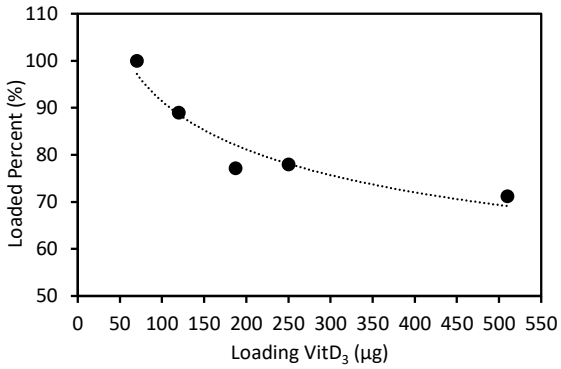

Figure 4.17. Encapsulation efficiency of $VitD_3$ loaded liposomes.

4.11. Fucoidan Coating on Liposomes

In this study, liposomes were coated by fucoidan (FUC) to promote targeted delivery of $VitD_3$. Fucoidan has a strong affinity to the p-selectin overexpressed in breast cancer cells. Fucoidan coating was performed onto the liposomes with different DSTAP mole% contents on the liposomes. Liposomes were aliquoted into the tubes and different amounts of Fucoidan was added to each aliquot in the tubes. Average size and zeta potentials of the liposomes were measured after each addition.

Figure 4.18 shows the pictures of vials after sequential addition of fucoidan into PBS solution, bare liposomes, and DSTAP containing liposomes. As shown in Figure 4.18.(a), the fucoidan solution was almost homogenous at low concentrations. When the fucoidan concentration was increased, the solution became yellowish and more viscous, which are the characteristic of fucoidan in aqueous solution. Figure 4.18.(b) shows the fucoidan addition to bare liposomes. Because the bare liposomes were almost neutral or slightly negatively charged (about -3 mV), the fucoidan solution did not affect their appearance considerably. Figure 4.18.(c) shows the fucoidan addition to positively charged liposomes containing DSTAP on their surface. As shown in the figure, there seems to be clear liposome suspensions in the first two vials. Thereafter, the vials were seen to contain almost aggregated and viscous moieties on the surface of the vial, indicating that some of the liposomes aggregated in the presence of electrolytic fucoidan chains. Lai et al. also observed a phase separation when fucoidan was added on nanoemulsions and nanoparticles over time (Lai et al., 2020). They stated that the stability of emulsions changed due to the characteristics of the nanoparticles used. They suggested using poly (lactic-co-glycolic acid) (PLGA) in order to maintain stability.

Figure 4.18. Sequential addition of fucoidan to (a) PBS buffer solution, (b) bare liposomes, (c) liposomes containing 10mole% DSTAP. FUC additions were done by 30-minute time intervals.

Figure 4.19 shows the zeta potential and sizes after sequential addition of fucoidan to the liposomes containing different DSTAP mole%. As shown in Figure 4.19.(a), the liposomes' surface charge decreased gradually upon controlled addition of fucoidan. The zeta potential for bare liposomes and fucoidan itself in the PBS buffer were also shown. The bare liposomes showed slightly negative charge with a zeta potential value of -3 mV. The fucoidan in the PBS solution also showed slightly negative charge with zeta potential values of about -3 mV. With increasing DSTAP mole% in the liposomes, their surface charge became more positively charged. Therefore, upon addition of fucoidan, the surface charge decreased gradually until the surface charge became neutralized and then decreased further down to negatively charge. These negative charges were different than the free fucoidan in PBS indicating that the fucoidan molecules probably aligned on the surface of the liposomes forming fringes. Therefore, much less negatively charged zeta potential values were measured. Another point in these titration studies was that the amount of fucoidan loaded onto liposomes increased with increasing amount of DSTAP in the liposomes.

Figure 4.19.(b) shows the measured average sizes for the liposomes after sequential addition of fucoidan solution. As shown in the figure, the size of the bare liposomes was about 200 nm and increased slightly with fucoidan addition. Because fucoidan chains binds to the liposome surface electrostatically, this slight increase can be attributed to either fucoidan itself or the change in the medium properties such as viscosity due to FUC addition. Surprisingly, the sizes of fucoidan solution in PBS were about 1000 nm which were much more than the sizes measured for the bare liposomes. The sizes of charged liposomes were about 4-6 μm with the addition of fucoidan. Increase in size of the positively charged liposomes at low amounts of fucoidan may be resulting from the bridging flocculation due to incomplete coating of liposomes surface. At excess amounts of FUC, bridging of the liposomes could also happen due to the effect, called, depletion flocculation. Therefore, determination of optimum amount of FUC is very important to avoid bridging. It is also possible that FUC solution could be causing fringes on the liposomes elongating the fucoidan chains from the surfaces of liposomes causing such larger liposome sizes.

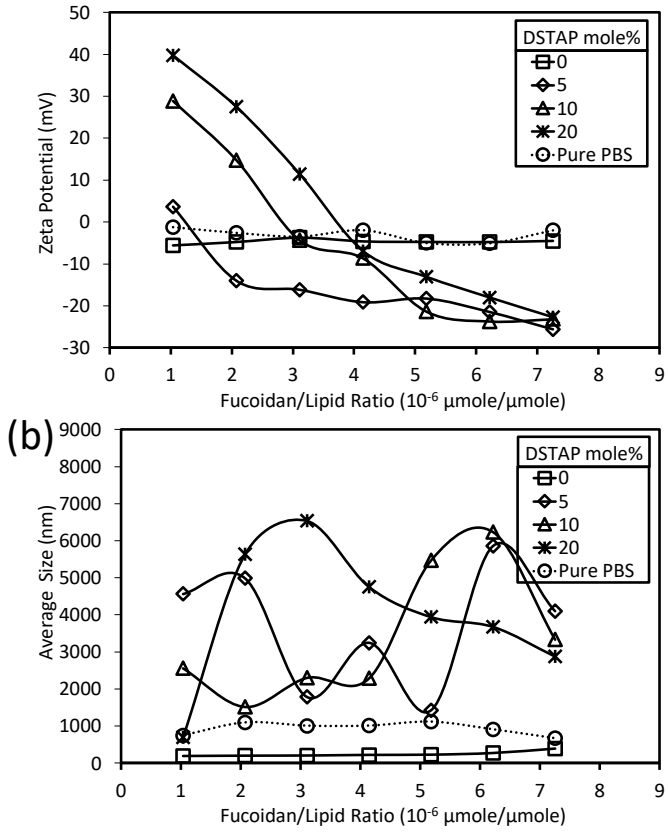

Figure 4.19. Effect of fucoidan on (a) zeta potential and (b) size of liposomes at different DSTAP mole%.

Addition of excess fucoidan to the liposomes made them to coagulated and finally sink after 24 hours of storage at 4 ºC in the fridge (Figure 4.20). As shown in the figure, some of the bare liposomes were still suspended in the suspension and charged liposomes were seen to sink. Therefore, there is a necessity that the fucoidan amount is to be optimized to make stable liposomes coated with fucoidan.

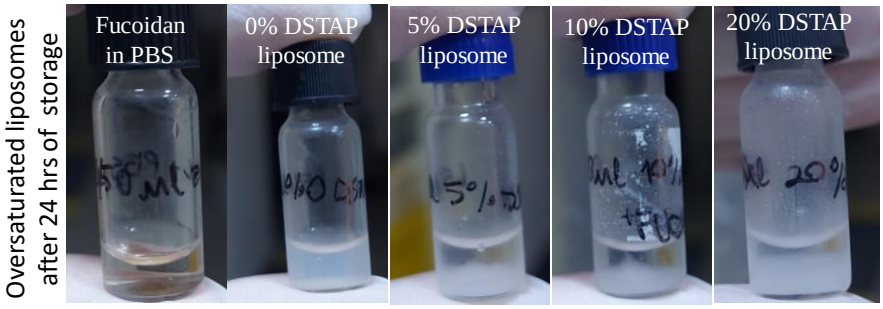

Figure 4.20. Phase separations of FUC added liposomes after 24 hours of storage at 4 °C.

4.12. VitD$_3$ Pretreatment on MDA-MB-231 Cells

The effect of VitD$_3$ on the cell viability was studied. Cells were incubated in wells. Average viable cell counts per square was calculated as 760.000 cell/ml for cell cultivation as 38 cells x 2 x 10^4 = 760.000 cell/ml. MTT results for cholecalciferol (VitD$_3$) treated (24-, 48- and 72-hours) well plates were shown in Figure 4.21. As shown in the figure, there were not a significant cell death in all groups with different VitD$_3$ concentrations during the experiment. It seems that VitD$_3$ concentrations up to 100 µM did not have any effect on the MDA-MB-231 breast cancer cells. Since VitD$_3$ is hydrophobic molecule, it was not expected to have a significant impact on tumor cells, because only the active form calcitriol can bind with the VitDR and shows an anti-cancer effect. Also, Wilhelm et al. pretreated MDA-MB-231 cancer cells with VitD$_3$ before paclitaxel (PTX) treatment and according to their results, VitD$_3$ did not affect the cell viability either (Wilhelm et al., 2018).

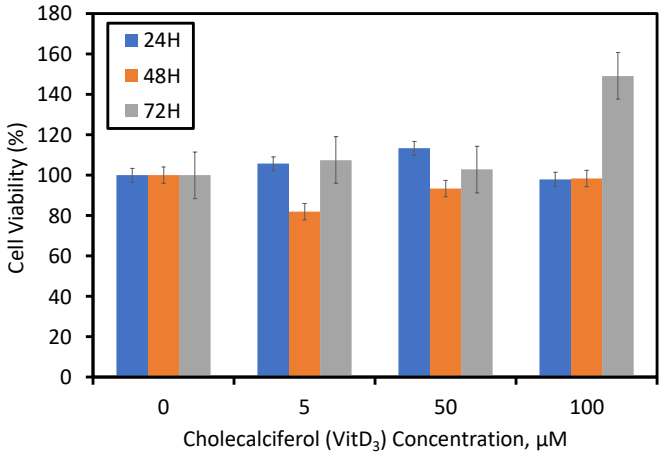

Figure 4.21. Cell viability of $VitD_3$ treated MDA-MB-231 cells in 24-, 48-, and 72 hours.

The effect of $VitD_3$ on cell viability with DOX treatment was studied. Figure 4.22 shows the cell viabilities in the presence of free DOX and free $VitD_3$ after 24-, 48- and 72-hours determined by MTT assay. As seen in the figure, in the presence of no DOX, while $VitD_3$ caused cell proliferation at low concentrations, it inhibited the cell viability relatively above 12.5 µg. In the DOX treatment in the presence of $VitD_3$, a decrease in cell viability was observed with increasing $VitD_3$ amount. This effect was more pronounced at increased DOX concentration. The effect of incubation time on cell viability however was not orderly. According to the study by Khriesha et al. on different $VitD_3$ concentration treatments to MCF-7 breast cancer cells, $VitD_3$ was inhibited the cell viability at 104-64-59 µM concentration groups (Khriesha et al., 2021), suggesting concentration depended cell viability inhibition of $VitD_3$. Combination of $VitD_3$ with 0.1 µM and 1 µM DOX data also showed that efficacy of DOX increased when it was combined with higher $VitD_3$ concentrations. According to the study by Guo et al. on $VitD_3$ combined treatment with metformin to MDA-MB-231 breast cancer cell, $VitD_3$ enhanced the apoptotic effect of metformin on cells and the effect of anti-cancer drug (Guo et al., 2015).

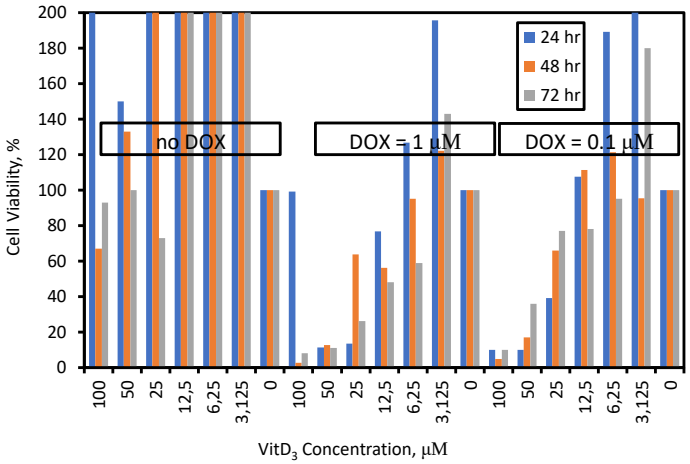

Figure 4.22. Cell viability of DOX and $VitD_3$ treated MDA-MB-231 cells.

4.13. Effect of Fucoidan Coated and $VitD_3$ Loaded Liposomes on Cell Viability

Effect of $VitD_3$ loaded liposomes and fucoidan coated $VitD_3$ loaded liposomes on cell viability were studied. First, $VitD_3$ was loaded within liposomes at different contents. Each liposome was added to MD-MBA-231 cell culture keeping the total liposome suspension volume the same. Figure 4.23.(a) shows the cell viability upon addition of liposomes containing different $VitD_3$ to the cell culture after 24, 48, and 72 hours. Also, one of the $VitD_3$ loaded liposomes, containing $VitD_3$ with 0.51 mg/ml, was diluted to different portions and added to the cell culture. As shown in the figure, cell viability decreased with increasing $VitD_3$ content in the liposomes while liposome volume was constant. Similar effect was observed when increasing the volumes, and therefore the amount of $VitD_3$ content, of the same $VitD_3$ loaded liposomes added to the cell cultivation. It is interesting to note that the cell viability increased on the second day and decreased on the third day in the presence of $VitD_3$.

The effect of fucoidan coating on the $VitD_3$ loaded liposomes were also investigated on the MD-MBA-231 cell cultures. 0.35 mg/ml fucoidan solution was coated onto liposomes containing different $VitD_3$ contents. Also, this fucoidan solution was diluted to different concentrations and they were coated on the aliquots of 0.51 mg/ml $VitD_3$ coated liposomes. Figure 4.23.(b) shows the cell viability upon addition of liposomes containing different $VitD_3$ contents and coated with the same amount of fucoidan. The figure also shows the cell viability upon addition of liposomes containing constant amount of $VitD_3$ but coated with different amounts of fucoidan. As shown in the

figure, cells were not affected considerably on the first day upon addition of fucoidan coated and $VitD_3$ loaded liposomes. However, cell viability decreased on the second and third day as the cell cultivation progressed. While lower concentrations of fucoidan did not affect the cell viability significantly, increasing $VitD_3$ content of liposomes had a dramatic effect on the cell viability in the presence of fucoidan coated liposomes. The 0.35 mg/ml fucoidan coated and 0.51 mg/ml $VitD_3$ loaded liposomes showed the most significant effect on the cell viability, almost comparable to DOX loaded liposomes with and without FUC coating Figure 4.23.(b).

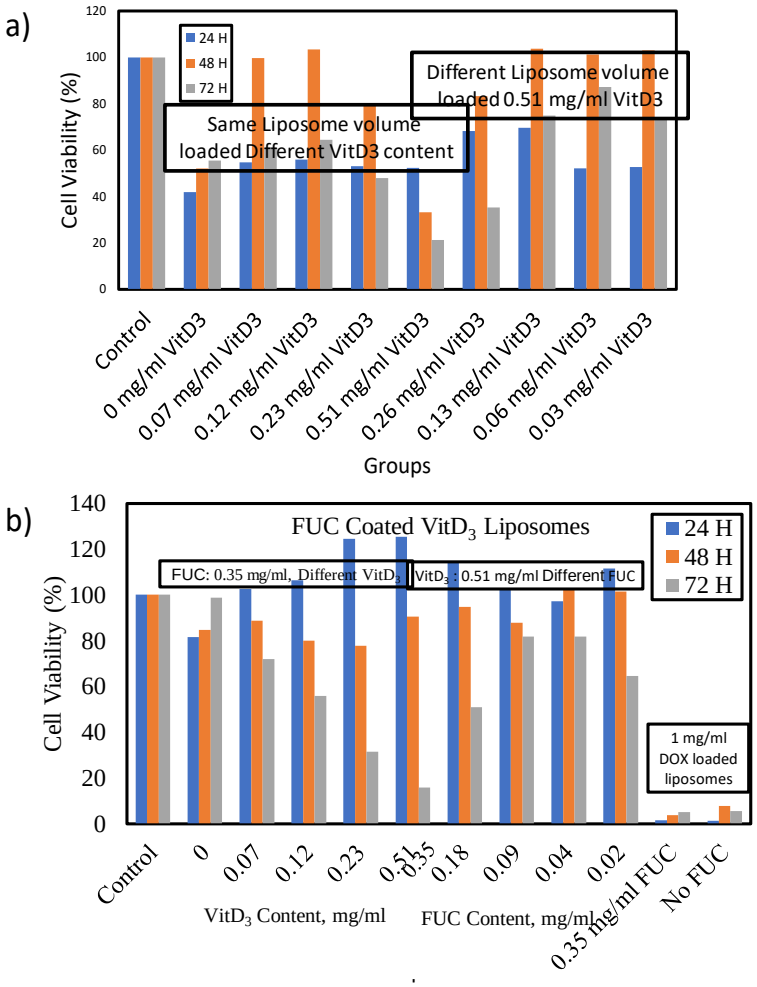

Figure 4.23. Effect of liposomal $VitD_3$ on cell viability (a) only $VitD_3$ loaded liposomes, (b) FUC coated $VitD_3$ liposomes. Also, the effect of DOX loaded, and DOX loaded fucoidan coated liposomes were shown.

CHAPTER 5

CONCLUSIONS

The aim of this study was to increase the bioavailability of cholecalciferol ($VitD_3$) by nano-sized delivery systems. For this purpose, liposome was considered as the drug delivery vehicles for $VitD_3$ because of its hydrophobic molecule carriable structure. DSPC, cholesterol and DSTAP were used for liposome composition and $VitD_3$ was loaded passively. First, to determine the optimum DSTAP percentage in the liposome formulation for FUC coating, size and zeta potential of liposomes with different DSTAP percentage were measured. Zeta potential of the liposomes increased with increasing DSTAP up to 15 %, then almost leveled off afterwards at zeta potential around 27 mV All liposomes exhibited a size around 200 nm, regardless of the DSTAP content, indicating that pore-size of the polycarbonate membrane during the extrusion process determined the final size of the liposomes.

To the liposomes composed of DSPC/Cholesterol/DSTAP at molar ratio of 55:30:15, $VitD_3$ was loaded passively. It was seen that zeta potential of the $VitD_3$ liposomes decreased with increasing $VitD_3$ mole% while their size remained almost unchanged. Quantification of loaded $VitD_3$ into liposomes was performed by UV spectrophotometry at 265 nm using ethanol as solvent. It was found that the absorbance of the $VitD_3$ was affected by the background absorbance resulting from PBS from the liposomal solution when mixed with ethanol. A method was developed by subtracting the background spectra from the sample spectra and found that $VitD_3$ loaded into liposomes can be quantified by UV spectrophotometer as long as the ethanol content is higher than 90 moles % in the measurement medium. The encapsulation efficiency of liposomes was determined by centrifugation technique and seen that it decreased with the increasing amount of $VitD_3$ added to the liposomal formulation. The decrease in encapsulation efficiency was attributed to loss of $VitD_3$ during the extrusion process being retained by the membrane.

Fucoidan (FUC) coating was done on the liposomes with different DSTAP percentages. With the gradual addition of fucoidan, there was a decrease in the zeta potential of the liposomes, going to neutral and eventually negative zeta potentials, indicating the coating of the positively charged liposome surface with negatively charged fucoidan. The amount of fucoidan loaded onto liposomes was found to increase with increasing amount of DSTAP in the liposomes.

Cell viability studies indicated that free $VitD_3$ in the concentrations up to 100 μM did not have any effect on the MDA-MB-231 breast cancer cells. In the DOX treatment with the presence of $VitD_3$, cell viability decreased with increasing $VitD_3$ amount. This effect was much more pronounced when DOX concentration increased from 0.1 μM to 1 μM. The effect of incubation time on cell viability however was not orderly. In the presence of no DOX, VitD3 was effective to prevent cell proliferation above the amounts higher than 12.5 μg while it caused cell proliferation below that.

Effect of $VitD_3$ loaded and fucoidan coated liposomes on the cell viability of MDA-MB-231 cancer cells was also investigated and more pronounced effects was observed with the liposomal $VitD_3$. Cell viability indicated a decrease with increasing encapsulated $VitD_3$ in the liposomes. Similar effect was observed when increasing the volumes, and therefore the amount of $VitD_3$ content, of the same $VitD_3$ loaded liposomes added to the cell cultivation. Constant $VitD_3$ containing liposomes coated with fucoidan was more effective on the cells after the first day, causing the cell non-proliferation. $VitD_3$-loaded and FUC-coated liposomes indicated almost comparable effect with the DOX-loaded liposomes with and without FUC coating. Overall, the results suggested that $VitD_3$ can be used as a combined therapy with DOX to increase therapeutic potential of the latter. These results imply that their encapsulation into liposomes followed by fucoidan coating can help the all-cargo to be delivered to the cancerous tissues of interest and thus create a combined effect at the target site.

REFERENCES

A, I., PO, U., TA, A., & NO, B. (2021). Cholesterol and Its Implications- a Review. *Universal Journal of Pharmaceutical Research*, *January*. https://doi.org/10.22270/ujpr.v5i6.513

Abreu Domingues, N. J. (2013). *Carrier Systems for Vitamin D*. *July*.

Al-Hajj, M., Wicha, M. S., Benito-Hernandez, A., Morrison, S. J., & Clarke, M. F. (2003). Prospective identification of tumorigenic breast cancer cells. *Proceedings of the National Academy of Sciences of the United States of America*, *100*(7), 3983–3988. https://doi.org/10.1073/pnas.0530291100

Apostolova, E., Lukova, P., Baldzhieva, A., Katsarov, P., Nikolova, M., Iliev, I., Peychev, L., Trica, B., Oancea, F., Delattre, C., & Kokova, V. (2020). of Fucoidan : A Review. *Polymers*, *12*, *2338*, 1–22.

Baggerly, C. A., Cuomo, R. E., French, C. B., Garland, C. F., Gorham, E. D., Grant, W. B., Heaney, R. P., Holick, M. F., Hollis, B. W., McDonnell, S. L., Pittaway, M., Seaton, P., Wagner, C. L., & Wunsch, A. (2015). Sunlight and Vitamin D: Necessary for Public Health. *Journal of the American College of Nutrition*, *34*(4), 359–365. https://doi.org/10.1080/07315724.2015.1039866

Bischoff-Ferrari, H. (2009). Vitamin D: What is an adequate vitamin D level and how much supplementation is necessary? *Best Practice and Research: Clinical Rheumatology*, *23*(6), 789–795. https://doi.org/10.1016/j.berh.2009.09.005

Buras, R. R., Schumaker, L. M., Davoodi, F., Brenner, R. V., Shabahang, M., Nauta, R. J., & Evans, S. R. T. (1994). Vitamin D receptors in breast cancer cells. *Breast Cancer Research and Treatment*, *31*(2–3), 191–202. https://doi.org/10.1007/BF00666153

Carvalho, C., Santos, R., Cardoso, S., Correia, S., Oliveira, P., Santos, M., & Moreira, P. (2009). Doxorubicin: The Good, the Bad and the Ugly Effect. *Current Medicinal Chemistry*, *16*(25), 3267–3285. https://doi.org/10.2174/092986709788803312

Chen, P. s., Lane, K., Terepka, A. R., & Marsh, A. (1965). Studies of the and Extractability of Vitamin S . CHEN , JR ., A . RAYMOND Vitamin D3 is potentially unstable and , as evidenced by poor recoveries from various systems (6 , 7) even when added in vitro , can be destroyed by various experimental condition. *Analytical Biochemistry*, *434*(10), 421–434.

Citkowska, A., Szekalska, M., & Winnicka, K. (2019). Possibilities of fucoidan utilization in the development of pharmaceutical dosage forms. *Marine Drugs*, *17*(8). https://doi.org/10.3390/md17080458

Dabbas, S., Kaushik, R. R., Dandamudi, S., Kuesters, G. M., & Campbell, R. B. (2008). Importance of the liposomal cationic lipid content and type in tumor vascular targeting: Physicochemical characterization and in vitro studies using human primary and transformed endothelial cells. *Endothelium: Journal of Endothelial Cell Research*, *15*(4), 189–201. https://doi.org/10.1080/10623320802228583

Dalmoro, A., Bochicchio, S., Lamberti, G., Bertoncin, P., Janssens, B., & Barba, A. A. (2019). Micronutrients encapsulation in enhanced nanoliposomal carriers by a novel preparative technology. *RSC Advances*, *9*(34), 19800–19812. https://doi.org/10.1039/c9ra03022k

Ecacc, M.-. (2022). MCF-7 Cell line profile. *ECACC, European Collection of Authenticated Cell Cultures*, *4*(92020424), 1–2. https://www.phe-culturecollections.org.uk/media/130237/mcf7-cell-line-profile.pdf

El-Sharkawy, A., & Malki, A. (2020). Vitamin D signaling in inflammation and cancer: Molecular mechanisms and therapeutic implications. *Molecules*, *25*(14), 1–31. https://doi.org/10.3390/molecules25143219

Forrest, K. Y. Z., & Stuhldreher, W. L. (2011). Prevalence and correlates of vitamin D deficiency in US adults. *Nutrition Research*, *31*(1), 48–54. https://doi.org/10.1016/j.nutres.2010.12.001

Glowka, E., Stasiak, J., & Lulek, J. (2019). Drug delivery systems for vitamin D supplementation and therapy. *Pharmaceutics*, *11*(7). https://doi.org/10.3390/pharmaceutics11070347

Gonnet, M., Lethuaut, L., & Boury, F. (2010). New trends in encapsulation of liposoluble vitamins. *Journal of Controlled Release*, *146*(3), 276–290. https://doi.org/10.1016/j.jconrel.2010.01.037

Goubran, H. A., Kotb, R. R., Stakiw, J., Emara, M. E., & Burnouf, T. (2008). *Cancer growth and metastasis*. 9–18. https://doi.org/10.4137/CGM.S11285.RECEIVED

Grant, W. B., & Holick, M. F. (2005). Benefits and requirements of vitamin D for optimal health: A review. *Alternative Medicine Review*, *10*(2), 94–111.

Grant, W. B., Lahore, H., McDonnell, S. L., Baggerly, C. A., French, C. B., Aliano, J. L., & Bhattoa, H. P. (2020). Evidence that vitamin d supplementation could reduce risk of influenza and covid-19 infections and deaths. *Nutrients*, *12*(4), 1–19. https://doi.org/10.3390/nu12040988

Guo, L. S., Li, H. X., Li, C. Y., Zhang, S. Y., Chen, J., Wang, Q. L., Gao, J. M., Liang, J. Q., Gao, M. T., & Wu, Y. J. (2015). Synergistic antitumor activity of vitamin D3 combined with metformin in human breast carcinoma MDA-MB-231 cells involves m-TOR related signaling pathways. *Pharmazie*, *70*(2), 117–122. https://doi.org/10.1691/ph.2015.4535

Healthy, C., Piotrowska, A., Kłopotowska, D., & Dzi, P. (2020). *Gland Tumor-Bearing Mice*. *25*.

Ilie, P. C., Stefanescu, S., & Smith, L. (2020). The role of vitamin D in the prevention of coronavirus disease 2019 infection and mortality. *Aging Clinical and Experimental Research*, *32*(7), 1195–1198. https://doi.org/10.1007/s40520-020-01570-8

Jafari, M., Sriram, V., Xu, Z., Harris, G. M., & Lee, J. Y. (2020). Fucoidan-Doxorubicin Nanoparticles Targeting P-Selectin for Effective Breast Cancer Therapy. *Carbohydrate Polymers*, *249*(May), 116837. https://doi.org/10.1016/j.carbpol.2020.116837

Jäpelt, R. B., & Jakobsen, J. (2013). Vitamin D in plants: A review of occurrence, analysis, and biosynthesis. *Frontiers in Plant Science*, *4*(MAY). https://doi.org/10.3389/fpls.2013.00136

Kadappan, A. S. (2019). *ScholarWorks @ UMass Amherst The Efficacy of Nanoemulsion-Based Delivery Systems to Improve Vitamin D3 Bioaccessibility and Bioavailability The Efficacy of Nanoemulsion-Based Delivery Systems to Improve Vitamin D 3 Bioaccessibility and Bioavailability Sub*. *July*.

Khriesha, A., Bustan Ji, Y., Farha, R. A., Al-Abbasi, R., & Abu-Irmaileh, B. (2021). Evaluation of the potential anticancer activity of different vitamin D metabolites on colorectal and breast cancer cell lines. *Hormone Molecular Biology and Clinical Investigation*, *42*(1), 3–9. https://doi.org/10.1515/hmbci-2020-0045

Kutlehria, S., Behl, G., Patel, K., Doddapaneni, R., Vhora, I., Chowdhury, N., Bagde, A., & Singh, M. (2018). Cholecalciferol-PEG Conjugate Based Nanomicelles of Doxorubicin for Treatment of Triple-Negative Breast Cancer. *AAPS PharmSciTech*, *19*(2), 792–802. https://doi.org/10.1208/s12249-017-0885-z

Kylin, H. (1913). Zur Biochemie der Meeresalgen. *Hoppe-Seyler's Zeitschrift Fur Physiologische Chemie*, *83*(3), 171–197. https://doi.org/10.1515/bchm2.1913.83.3.171

Lai, Y. H., Chiang, C. S., Hsu, C. H., Cheng, H. W., & Chen, S. Y. (2020). Development and characterization of a fucoidan-based drug delivery system by using hydrophilic anticancer polysaccharides to simultaneously deliver hydrophobic anticancer drugs. *Biomolecules*, *10*(7), 1–18. https://doi.org/10.3390/biom10070970

Li, B., Lu, F., Wei, X., & Zhao, R. (2008). *Fucoidan: Structure and Bioactivity*. 1671–1695. https://doi.org/10.3390/molecules13081671

Liang, R., Bao, Z., Su, B., Xing, H., & Ren, Q. (2012). *Ruisi Liang, Zongbi Bao, * Baogen Su, Huabin Xing, and Qilong Ren*.

Lopes, N., Sousa, B., Martins, D., Gomes, M., Vieira, D., Veronese, L. A., Milanezi, F., Paredes, J., Costa, J. L., & Schmitt, F. (2010). Alterations in Vitamin D signalling and metabolic pathways in breast cancer progression: A study of VDR, CYP27B1 and CYP24A1 expression in benign and malignant breast lesions Vitamin D pathways unbalanced in breast lesions. *BMC Cancer*, *10*. https://doi.org/10.1186/1471-2407-10-483

Matsen, C. B., & Neumayer, L. A. (2013). Breast cancer: A review for the general surgeon. *JAMA Surgery*, *148*(10), 971–979. https://doi.org/10.1001/jamasurg.2013.3393

Maurya, V. K., & Aggarwal, M. (2017). Enhancing Bio-Availability of Vitamin D by Nano-Engineered Based Delivery Systems- An Overview. *International Journal of Current Microbiology and Applied Sciences*, *6*(7), 340–353. https://doi.org/10.20546/ijcmas.2017.607.040

Maurya, V. K., Bashir, K., & Aggarwal, M. (2020). Vitamin D microencapsulation and fortification: Trends and technologies. *Journal of Steroid Biochemistry and Molecular Biology*, *196*(October), 105489. https://doi.org/10.1016/j.jsbmb.2019.105489

Medeiros, J. F. P., de Oliveira Borges, M. V., Soares, A. A., dos Santos, J. C., de Oliveira, A. B. B., da Costa, C. H. B., Cruz, M. S., Bortolin, R. H., de Freitas, R. C. C., Dantas, P. M. S., Hirata, M. H., Silbiger, V. N., & Luchessi, A. D. (2020). The impact of vitamin D supplementation on VDR gene expression and body composition in monozygotic twins: randomized controlled trial. *Scientific Reports*, *10*(1), 1–10. https://doi.org/10.1038/s41598-020-69128-2

Media, I. R. (2014). *TransfeX ™ Transfection of Plasmid DNA into HEK293T / 17*. *17*, 1–3.

Mohammadi, M., Ghanbarzadeh, B., & Hamishehkar, H. (2014). Formulation of nanoliposomal vitamin D3 for potential application in beverage fortification. *Advanced Pharmaceutical Bulletin*, *4*(Suppl 2), 569–575. https://doi.org/10.5681/apb.2014.084

Muscogiuri, G. (2020). Introduction to Vitamin D: current evidence and future directions. *European Journal of Clinical Nutrition*, *74*(11), 1491–1492. https://doi.org/10.1038/s41430-020-00770-9

Novoyatleva, T., Kojonazarov, B., Owczarek, A., Veeroju, S., Rai, N., Henneke, I., Böhm, M., Grimminger, F., Ghofrani, H. A., Seeger, W., Weissmann, N., & Schermuly, R. T. (2019). Evidence for the fucoidan/p-selectin axis as a therapeutic target in hypoxia-induced pulmonary hypertension. *American Journal of Respiratory and Critical Care Medicine*, *199*(11), 1407–1420.

https://doi.org/10.1164/rccm.201806-1170OC

Patel, J. (1996). Liposomal doxorubicin: Doxil®. *Journal of Oncology Pharmacy Practice*, *2*(4), 201–210. https://doi.org/10.1177/107815529600200402

Ramalho, M. J., Coelho, M. A. N., & Pereira, M. C. (2017). Nanoparticles for Delivery of Vitamin D: Challenges and Opportunities. *A Critical Evaluation of Vitamin D - Clinical Overview*. https://doi.org/10.5772/64516

Renu, K., V.G., A., Tirupathi, T. P., & Arunachalam, S. (2018). Molecular mechanism of doxorubicin-induced cardiomyopathy – An update. In *European Journal of Pharmacology* (Vol. 818). https://doi.org/10.1016/j.ejphar.2017.10.043

Sabzichi, M., Mohammadian, J., Mohammadi, M., Jahanfar, F., Movassagh Pour, A. A., Hamishehkar, H., & Ostad-Rahimi, A. (2017). Vitamin D-Loaded Nanostructured Lipid Carrier (NLC): A New Strategy for Enhancing Efficacy of Doxorubicin in Breast Cancer Treatment. *Nutrition and Cancer*, *69*(6), 840–848. https://doi.org/10.1080/01635581.2017.1339820

Shafei, A., El-Bakly, W., Sobhy, A., Wagdy, O., Reda, A., Aboelenin, O., Marzouk, A., El Habak, K., Mostafa, R., Ali, M. A., & Ellithy, M. (2017). A review on the efficacy and toxicity of different doxorubicin nanoparticles for targeted therapy in metastatic breast cancer. *Biomedicine and Pharmacotherapy*, *95*(September), 1209–1218. https://doi.org/10.1016/j.biopha.2017.09.059

Smith, M. C., Crist, R. M., Clogston, J. D., & McNeil, S. E. (2017). Zeta potential: a case study of cationic, anionic, and neutral liposomes. *Analytical and Bioanalytical Chemistry*, *409*(24), 5779–5787. https://doi.org/10.1007/s00216-017-0527-z

Sun, Y. S., Zhao, Z., Yang, Z. N., Xu, F., Lu, H. J., Zhu, Z. Y., Shi, W., Jiang, J., Yao, P. P., & Zhu, H. P. (2017). Risk factors and preventions of breast cancer. *International Journal of Biological Sciences*, *13*(11), 1387–1397. https://doi.org/10.7150/ijbs.21635

Tyler, H., Lloyd, R. A. Y. D., & Zundel, W. S. (1968). *Frank h. 220*(c), 1–2.

Umar, M., Sastry, K. S., Al Ali, F., Al-Khulaifi, M., Wang, E., & Chouchane, A. I. (2018). Vitamin D and the Pathophysiology of Inflammatory Skin Diseases. *Skin Pharmacology and Physiology*, *31*(2), 74–86. https://doi.org/10.1159/000485132

van Weelden, G., Bobi, M., Okła, K., van Weelden, W. J., Romano, A., & Pijnenborg, J. M. A. (2019). Fucoidan structure and activity in relation to anti-cancer mechanisms. *Marine Drugs*, *17*(1). https://doi.org/10.3390/md17010032

Voutsadakis, I. A. (2020). Vitamin D receptor (VDR) and metabolizing enzymes CYP27B1 and CYP24A1 in breast cancer. *Molecular Biology Reports*, *47*(12), 9821–9830. https://doi.org/10.1007/s11033-020-05780-1

Wilhelm, C. A., Clor, Z. J., & Kelts, J. L. (2018). Effect of Vitamin D on paclitaxel efficacy in triple-negative breast cancer cell lines. *Anticancer Research*, *38*(9), 5043–5048. https://doi.org/10.21873/anticanres.12823

Wolfram, J., Suri, K., Yang, Y., Shen, J., Celia, C., Fresta, M., Zhao, Y., Shen, H., & Ferrari, M. (2014). Shrinkage of pegylated and non-pegylated liposomes in serum. *Colloids and Surfaces B: Biointerfaces*, *114*, 294–300. https://doi.org/10.1016/j.colsurfb.2013.10.009

Zheng, W., Duan, B., Zhang, Q., Ouyang, L., Peng, W., Qian, F., Wang, Y., & Huang, S. (2018). Vitamin D-induced vitamin D receptor expression induces tamoxifen sensitivity in MCF-7 stem cells via suppression of Wnt/-catenin signaling. *Bioscience Reports*, *38*(6). https://doi.org/10.1042/BSR20180595